Computer Simulations in Solid-State NMR. I. Spin Dynamics Theory

MATTIAS EDÉN

*Physical Chemistry Division, Arrhenius Laboratory, Stockholm University, SE-*106 91 *Stockholm, Sweden*

ABSTRACT: This article is the first in a series of publications that discuss the basics of the writing of computer programs for simulating solid-state NMR experiments with static and rotating samples. The present article gives an account of the relevant NMR theory needed for writing NMR simulation computer codes. The concept of irreducible spherical tensors is reviewed, as is how it may be used to construct Hamiltonians that represent the various NMR interactions. The spin dynamics that links the Hamiltonian to the time evolution of the nuclear spins and the detection of the NMR time-domain signal is discussed for static and rotating solids, as well as the relationship between the form of the Hamiltonian and the resulting NMR spectrum. Concepts Magn Reson Part A 17A: 117–154, 2003

KEY WORDS: solid-state NMR; numerical simulation; static solids; magic-angle spinning; dynamically inhomogeneous Hamiltonian; spherical tensor

INTRODUCTION

The analysis of most NMR experiments relies on numerical simulations. For example, numerical simulations are needed for extracting information about spin interaction parameters and molecular structure by means of iterative fitting of calculated NMR responses to experimental data. Computer modeling of experiments are also extensively used for testing and optimizing new NMR methodologies: through a computer program, it is straightforward to isolate and study the relative importance of various parameters affecting the NMR measurement. Such investigations may prove difficult or even impossible to carry out experimentally.

All NMR interactions have *anisotropic* contributions (*1–6*), which is clearly manifested in NMR experiments with solid samples. The NMR response of the interactions depends on the orientation of the molecule (containing the nuclear spins under study) with respect to the direction of the static magnetic field. Experiments are usually performed on powders comprising a large number of randomly oriented crystallites. The resulting NMR spectrum is then a superposition of the spectra from all crystallites. This gives powder spectra with NMR resonances spread over a large range of frequencies, as seen in Fig. 1(a).

In order to obtain high resolution NMR spectra from powders, experimental manipulations of the spins are often required, such as magic-angle spinning

Received 5 October 2001; revised 22 October 2002; accepted 20 November 2002

Correspondence to: Dr. M. Edén; E-mail: mattias@physc.su.se

Concepts in Magnetic Resonance Part A, Vol. 17A(1) 117–154 (2003)

Published online in Wiley InterScience (www.interscience.wiley.com). DOI 10.1002/cmr.a.10061

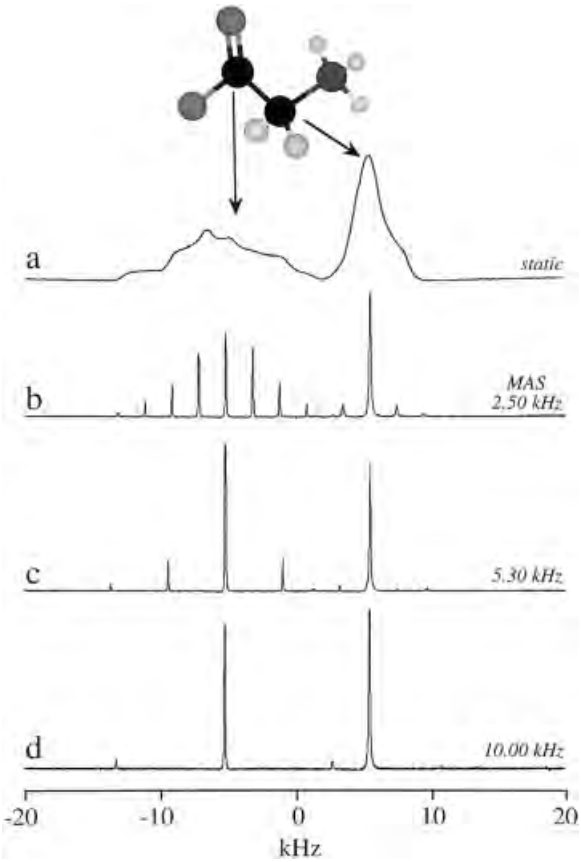

Figure 1 The experimental ^{13}C spectra of a powder of 99%-$^{13}C_2$-labeled glycine, acquired at a magnetic field of 9.4 T. High-power proton decoupling was employed during the acquisition. (a) The spectrum of a static sample. (b–d) Spectra for a sample rotating at the magic angle and recorded at a spinning frequency equal to (b) 2.50, (c) 5.30, and (d) 10.00 kHz.

(MAS) and/or techniques involving high power radio frequency (RF) field application (*1–5, 7, 8*). MAS is based on the idea that because the anisotropic interactions are orientation dependent, they may be removed by rapidly rotating the sample about the axis of the sample holder, which should be inclined at the "magic angle" $\theta_m = \arctan\sqrt{2}$ with respect to the static magnetic field direction. MAS diminishes the effects of the anisotropic interactions; and if the sample rotation is fast enough, they are averaged out completely, as shown in Fig. 1(d).

As a result of the time-dependent modulations, combined with the anisotropic nature of the spin interactions, numerical simulations of solid-state NMR experiments are quite demanding and generally require different computational techniques than those for isotropic liquids. Additional complications arise when simulating NMR responses from powders, because the calculation must then incorporate *powder averaging*, implying a summation of the signals from a large number of molecular orientations.

Over the last few years, simulations of solid-state NMR experiments have reached a high degree of sophistication. It is possible to simulate NMR signals by mimicking the experimental situation very closely, using a minimum of assumptions. For example, powder averaged MAS spectra from multiple-spin systems can be simulated in a few seconds or minutes on a personal computer, taking all relevant interactions of the spin system into account (*9–14*). Even powder averaged spectra for 2-dimensional experiments involving complex pulse sequences may be calculated within 1 h (*14–16*). This is a result of steadily increasing computer capabilities, combined with highly efficient general-purpose computational methods that have recently been introduced (*10–13, 15, 17–20*). There are simulation packages available for various solid-state NMR simulations (*21–23*). In particular, two very sophisticated simulation platforms, GAMMA (*24, 25*) and SIMPSON (*14, 26*), have found well-spread public usage.

The present article is the first in a series that seeks to outline how a numerical simulation program may be written for calculating NMR time-domain signals or frequency-domain spectra with emphasis on so-called *dynamically inhomogeneous* cases as defined by Maricq and Waugh (*27*). These correspond to evolution of the nuclear spins under either a time-independent Hamiltonian or a time-dependent Hamiltonian that commutes with itself at all times. This applies, for instance, to isolated spins and heteronuclear spin systems under MAS conditions. These articles may also be of interest to the users of already existing simulation software, because we discuss general aspects of utility when executing simulation programs.

Writing a numerical simulation program requires insight into the NMR theory underlying the description of the experiment, in particular, the form of the Hamiltonian under which the spins evolve. Moreover, it is necessary to have a systematic procedure for constructing the spin Hamiltonian for any given experiment. In this series of *Concepts* articles, we address the problem using the irreducible spherical tensor (IST) formalism (*1–5, 28, 29*). An explanation is made on how the Hamiltonian may be formed as a product of one IST (the "spatial tensor") that depends on the orientation of the molecule with respect to the magnetic field and another IST that is represented by spin operators. The IST formalism is highly suited for describing the response of NMR interactions to rotations of the sample, which is needed for the theoret-

ical, as well as numerical, treatment of MAS experiments.

A numerical simulation program for calculating the NMR time-domain signal or frequency-domain spectrum comprises the following main parts:

1. *Initialization.* For numerical simulations, it is first necessary to provide the program with input data characterizing the spin system and its interactions. Parameters describing the particular experimental situation are also required, such as the MAS frequency. Furthermore, the desired form of output of the calculation is needed, for example, the spectral window and frequency resolution. Simulations of complex experiments may require a large amount of input data. Once the necessary data are gathered, the spatial tensors and spin operators are constructed, as discussed in later sections.
2. *Spin dynamics calculation.* This is the heart of the simulation program, where typically 99% of the computational time is spent and finally results in the calculated NMR response. Calculating "spin dynamics" means finding how the spin density operator (which specifies the state of an ensemble of spin systems) evolves in time during the NMR experiment that is to be simulated. The nature of the spin dynamics is directly reflected in the NMR time-domain signal and spectrum. This article outlines a spin dynamics theory, which is examined in detail for spin systems evolving under dynamically inhomogeneous Hamiltonians. The relationship between the NMR spectrum and the particular type of Hamiltonian (time independent as in the case of a static solid or time periodic as in the case of MAS) is also examined.
3. *Postprocessing.* The final part of the simulation program may involve additional processing of the calculated NMR signal, such as applying broadening to the spectral peaks.

The numerical implementations of the spin dynamics calculations and postprocessing of the NMR signals will be discussed in the following article. We stress that this article only deals with calculation of the NMR response from a *single* molecular orientation (i.e., a single crystal). Simulations of time signals and spectra of powders require powder averaging. This stage of the simulation will be included in a following publication.

MATHEMATICAL CONCEPTS AND GENERAL CONVENTIONS

This section reviews basic mathematical tools employed in the formulation of spin dynamics theory. They are used later in the implementations of the computer codes in subsequent articles. The following references contain additional information on these topics: diagonalization of operators and exponential operators (*2–4, 6, 29, 30*); Fourier transformation (*4, 6, 30*); Euler angles, tensors, and rotations (*1, 4, 5, 29*).

Notation

Entities that may be represented as matrices (such as tensors and vectors) are set in boldface letters. Vectors are superscripted by single-headed arrows (e.g., $\vec{\mathbf{n}}$) and tensors by double-headed arrows (e.g., $\overleftrightarrow{\mathbf{A}}$). All operators are superscripted by a circumflex ($\hat{\mathbf{I}}_z$).

Components of vectors and tensors are italicized (e.g., V_z and A_{lm}); and, if the tensor components themselves are operators, they are set in bold letters (e.g., $\hat{\mathbf{T}}_{lm}$). We employ two alternative notations for matrix elements: in the outline of numerical algorithms, O_{jk} denotes the element of row j and column k of the operator $\hat{\mathbf{O}}$, evaluated in some basis set; and we also make frequent use of the Dirac (bracket) formalism (*2, 3, 29*). For a given basis, the relationship between the two notations is $O_{jk} \equiv \langle j|\hat{\mathbf{O}}|\mathrm{k}\rangle$.

An object A represented in a coordinate system (frame) F is denoted within brackets, and the frame label is superscript: $[A]^F$.

We also make a distinction between *points* in time, denoted t, and *time intervals* (i.e., differences between two points in time), denoted τ (*31*).

Diagonalization of Operators

An *Hermitian* operator (*2, 3, 6, 29*) is invariant to taking transpose and complex conjugate (together represented by the adjoint operation †)

$$\hat{\mathbf{A}} = \hat{\mathbf{A}}^{\dagger} \qquad [1]$$

Any Hermitian operator $\hat{\mathbf{A}}$ (e.g., the Hamiltonian $\hat{\mathbf{H}}$) may be diagonalized, that is, brought into a representation such that all its matrix elements are zero, except those on the diagonal. We denote this representation $\hat{\mathbf{A}}_{\mathrm{diag}}$. The particular basis where the operator is diagonal is called the *eigenbasis* of the operator. For an operator of dimensions $\mathcal{N} \times \mathcal{N}$, the eigenbasis is spanned by $\mathcal{N}$ orthonormal eigenstates (eigenvectors)

of $\hat{\mathbf{A}}$: $\{|1\rangle, |2\rangle, \ldots, |\mathcal{N}\rangle\}$. The orthonormality condition means that the scalar product between a state with itself is one and that between any two different states is zero:

$$\langle j|k\rangle = \delta(j, k) = \begin{cases} 1 & \text{if } j = k \\ 0 & \text{if } j \neq k \end{cases} \quad [2]$$

where δ represents the Kronecker δ function (*32*). Each of the eigenstates of $\hat{\mathbf{A}}$ obeys the following so-called *eigenequation* (*2–4, 6, 29*):

$$\hat{\mathbf{A}}|j\rangle = a_j|j\rangle \quad [3]$$

It means that if the operator acts on one of its eigenstates $|j\rangle$, the outcome is the *same* state, multiplied by a number a_j, called the *eigenvalue* of $\hat{\mathbf{A}}$ that corresponds to $|j\rangle$.

To diagonalize $\hat{\mathbf{A}}$, the operator that effects the transformation $\hat{\mathbf{A}} \rightarrow \hat{\mathbf{A}}_{\text{diag}}$ is needed. This operator is denoted $\hat{\mathbf{X}}$ and its matrix representation has the normalized eigenstates of $\hat{\mathbf{A}}$ as columns. In addition, $\hat{\mathbf{X}}$ is a *unitary* operator (*29*), which is defined as having the adjoint operator as its inverse (i.e., $\hat{\mathbf{X}}^\dagger = \hat{\mathbf{X}}^{-1}$), implying that

$$\hat{\mathbf{X}}\hat{\mathbf{X}}^\dagger = \hat{\mathbf{X}}^\dagger\hat{\mathbf{X}} = \hat{1} \quad [4]$$

where $\hat{1}$ is the *unity* operator, for which all matrix elements are zero, except those on the diagonal: $\langle j|\hat{1}|k\rangle = \delta(j, k)$. The diagonal matrix $\hat{\mathbf{A}}_{\text{diag}}$ may be obtained from the following operator "sandwich":

$$\hat{\mathbf{A}}_{\text{diag}} = \hat{\mathbf{X}}^\dagger\hat{\mathbf{A}}\hat{\mathbf{X}} \quad [5]$$

$$= \begin{pmatrix} a_1 & 0 & 0 & \cdots & 0 \\ 0 & a_2 & 0 & \cdots & 0 \\ 0 & 0 & a_3 & \cdots & 0 \\ \vdots & \vdots & \vdots & \ddots & \vdots \\ 0 & 0 & 0 & \cdots & a_{\mathcal{N}} \end{pmatrix} \quad [6]$$

A proof of Eq. [5] is given in Refs. (4, 29). Equation [6] may be expressed in the Dirac formalism as a sum of products of eigenvalues and projection operators.

$$\hat{\mathbf{A}}_{\text{diag}} = \sum_{j=1}^{\mathcal{N}} a_j|j\rangle\langle j| \quad [7]$$

where each operator $|j\rangle\langle j|$ projects a given state vector onto the eigenstate $|j\rangle$ (*2–4, 6, 29*). We may check that Eqs. [6] and [7] are equivalent by calculating the kth element of $\hat{\mathbf{A}}_{\text{diag}}$, that is, $(\hat{\mathbf{A}}_{\text{diag}})_{kk} = \langle k|\hat{\mathbf{A}}_{\text{diag}}|k\rangle$. Multiplying Eq. [7] from the left with $\langle k|$ and from the right with $|k\rangle$ gives

$$\langle k|\hat{\mathbf{A}}_{\text{diag}}|k\rangle = \langle k|\left(\sum_{j=1}^{\mathcal{N}} a_j|j\rangle\langle j|\right)|k \quad [8]$$

The Dirac formalism allows us to interpret each term of the right-hand side *either* as $a_j\langle k| \cdot |j\rangle\langle j| \cdot |k\rangle$ *or* as a product of two scalar products $a_j\langle k|j\rangle \cdot \langle j|k\rangle$ (*29*). Using the latter interpretation gives

$$\langle k|\hat{\mathbf{A}}_{\text{diag}}|k\rangle = \sum_{j=1}^{\mathcal{N}} a_j\langle k|j\rangle \cdot \langle j|k\rangle \quad [9]$$

$$= \sum_{j=1}^{\mathcal{N}} a_j\delta(j, k) \quad [10]$$

From the orthonormality of the eigenstates (Eq. [2]), all terms in the sum vanish, except for that with $j = k$, and we get $\langle k|\hat{\mathbf{A}}_{\text{diag}}|k\rangle = a_k$ as expected.

Equation [5] may be used to transform an arbitrary operator $\hat{\mathbf{B}}$ into the eigenbasis of $\hat{\mathbf{A}}$ according to (*29*)

$$\hat{\mathbf{B}} \rightarrow \hat{\mathbf{X}}^\dagger\hat{\mathbf{B}}\hat{\mathbf{X}} \quad [11]$$

Note, however, that *unless* $\hat{\mathbf{A}}$ and $\hat{\mathbf{B}}$ *share* the *same eigenbasis*, the operator $\hat{\mathbf{X}}^\dagger\hat{\mathbf{B}}\hat{\mathbf{X}}$ is *not* represented by a diagonal matrix (*29*).

Exponential Operators

In the following we frequently need to form the complex exponential $\exp\{i\hat{\mathbf{A}}\}$ of an Hermitian *operator* $\hat{\mathbf{A}}$. Just as the exponential of a real or complex *number* c may be calculated from a Taylor series

$$\exp\{c\} = 1 + c + \frac{1}{2!}c^2 + \frac{1}{3!}c^3 + \cdots + \frac{1}{N!}c^N + \cdots \quad [12]$$

an exponential operator may formally be interpreted as

$$\exp\{i\hat{\mathbf{A}}\} = \hat{1} + \hat{\mathbf{A}} + \frac{1}{2!}(i\hat{\mathbf{A}})^2 + \frac{1}{3!}(i\hat{\mathbf{A}})^3 + \cdots + \frac{1}{N!}(i\hat{\mathbf{A}})^N + \cdots \quad [13]$$

where $\hat{\mathbf{A}}^2 = \hat{\mathbf{A}} \cdot \hat{\mathbf{A}}$, and so forth. How is a power of an operator $\hat{\mathbf{A}}^N$ calculated for large N? Equation [5] is helpful because, for example, it may be exploited to obtain $\hat{\mathbf{A}}^3$ as follows:

$$\hat{\mathbf{A}}^3 = \hat{\mathbf{A}} \cdot \hat{\mathbf{A}} \cdot \hat{\mathbf{A}} = (\hat{\mathbf{X}}\hat{\mathbf{A}}_{\text{diag}}\hat{\mathbf{X}}^\dagger)(\hat{\mathbf{X}}\hat{\mathbf{A}}_{\text{diag}}\hat{\mathbf{X}}^\dagger)(\hat{\mathbf{X}}\hat{\mathbf{A}}_{\text{diag}}\hat{\mathbf{X}}^\dagger) \quad [14]$$

The right-hand side may be simplified by exploiting that $\hat{\mathbf{X}}$ is unitary and hence that the products $\hat{\mathbf{X}}^\dagger\hat{\mathbf{X}}$ cancel (Eq. [4]). Equation [14] then casts as

$$\hat{\mathbf{A}}^3 = \hat{\mathbf{X}}\hat{\mathbf{A}}^3_{\text{diag}}\hat{\mathbf{X}}^\dagger \quad [15]$$

Note that whenever $\hat{\mathbf{A}}_{\text{diag}}$ is diagonal, it may be directly raised to any power N according to

$$\hat{\mathbf{A}}^N_{\text{diag}} = \begin{pmatrix} a_1^N & 0 & 0 & \cdots & 0 \\ 0 & a_2^N & 0 & \cdots & 0 \\ 0 & 0 & a_3^N & \cdots & 0 \\ \vdots & 0 & 0 & \ddots & \vdots \\ 0 & 0 & 0 & \cdots & a_N^N \end{pmatrix} \quad [16]$$

From this follows that $\hat{\mathbf{A}}^3$ is formed by first calculating $\hat{\mathbf{A}}^3_{\text{diag}}$ and then multiplying it with $\hat{\mathbf{X}}$ from the left and $\hat{\mathbf{X}}^\dagger$ from the right.

When applying this strategy to Eq. [13], we obtain

$$\exp\{i\hat{\mathbf{A}}\} = \hat{1} + (i\hat{\mathbf{X}}\hat{\mathbf{A}}_{\text{diag}}\hat{\mathbf{X}}^\dagger) + \frac{1}{2!}(i\hat{\mathbf{X}}\hat{\mathbf{A}}_{\text{diag}}\hat{\mathbf{X}}^\dagger)^2 + \cdots + \frac{1}{N!}(i\hat{\mathbf{X}}\hat{\mathbf{A}}_{\text{diag}}\hat{\mathbf{X}}^\dagger)^N + \cdots \quad [17]$$

$$= \hat{1} + (i\hat{\mathbf{X}}\hat{\mathbf{A}}_{\text{diag}}\hat{\mathbf{X}}^\dagger) + \frac{1}{2!}(i\hat{\mathbf{X}}\hat{\mathbf{A}}^2_{\text{diag}}\hat{\mathbf{X}}^\dagger) + \cdots + \frac{1}{N!}(i\hat{\mathbf{X}}\hat{\mathbf{A}}^N_{\text{diag}}\hat{\mathbf{X}}^\dagger) + \cdots \quad [18]$$

Because each term is "sandwiched" by $\hat{\mathbf{X}}$ from the left and by $\hat{\mathbf{X}}^\dagger$ from the right, the sum may be factorized as

$$\exp\{i\hat{\mathbf{A}}\} = \hat{\mathbf{X}}\left(\hat{1} + i\hat{\mathbf{A}}_{\text{diag}} + \frac{1}{2!}(i\hat{\mathbf{A}}_{\text{diag}})^2 + \cdots + \frac{1}{N!}(i\hat{\mathbf{A}}_{\text{diag}})^N + \cdots\right)\hat{\mathbf{X}}^\dagger \quad [19]$$

The sum in the parentheses may be identified, according to Eq. [13], as the Taylor expansion of $\exp\{i\hat{\mathbf{A}}_{\text{diag}}\}$. In analogy with Eq. [16], the operator $\exp\{i\hat{\mathbf{A}}_{\text{diag}}\}$ is represented by a diagonal matrix with exponentials of eigenvalues on the diagonal:

$$\exp\{i\hat{\mathbf{A}}_{\text{diag}}\} = \begin{pmatrix} \exp\{ia_1\} & 0 & 0 & \cdots & 0 \\ 0 & \exp\{ia_2\} & 0 & \cdots & 0 \\ 0 & 0 & \exp\{ia_3\} & \cdots & 0 \\ \vdots & \vdots & \vdots & \ddots & \vdots \\ 0 & 0 & 0 & \cdots & \exp\{ia_N\} \end{pmatrix} \quad [20]$$

Inserting this result into Eq. [19] gives the following expression for the exponential operator $\exp\{i\hat{\mathbf{A}}\}$:

$$\exp\{i\hat{\mathbf{A}}\} = \hat{\mathbf{X}}\exp\{i\hat{\mathbf{A}}_{\text{diag}}\}\hat{\mathbf{X}}^\dagger \quad [21]$$

If the operator $\hat{\mathbf{A}}$ is Hermitian, the corresponding exponential operator $\exp\{i\hat{\mathbf{A}}\}$ is unitary (*6*, *29*). It follows that the inverse of the exponential operator is given by $\exp\{i\hat{\mathbf{A}}\}^{-1} = \exp\{-i\hat{\mathbf{A}}\}$. This may be verified by exploiting Eqs. [1] and [4] as follows:

$$\exp\{i\hat{\mathbf{A}}\}^{-1} = (\exp\{i\hat{\mathbf{A}}\})^\dagger = \exp\{(i)^\dagger\hat{\mathbf{A}}^\dagger\} = \exp\{-i\hat{\mathbf{A}}\} \quad [22]$$

Equation [21] is the route for obtaining exponential operators in numerical applications. The procedure to calculate $\exp\{i\hat{\mathbf{A}}\}$ is as follows:

1. diagonalize operator $\hat{\mathbf{A}}$ (i.e., find its eigenvalues and eigenvectors),
2. construct the matrix $\hat{\mathbf{X}}$ having the eigenvectors of $\hat{\mathbf{A}}$ as columns,
3. calculate the matrix of complex exponentials of the eigenvalues (Eq. [20]), and
4. form the product $\hat{\mathbf{X}}\exp\{i\hat{\mathbf{A}}_{\text{diag}}\}\hat{\mathbf{X}}^\dagger$ (Eq. [21]).

Fourier Series and Fourier Transforms

This section discusses basic concepts that are important when processing NMR responses, as well as in the mathematical formulation of the time evolution of nuclear spin systems. Here we also define parameters relevant for the experimental acquisition of NMR time-domain signals.

Fourier Series. A real- or complex-valued function $f(t)$ is said to be periodic with a characteristic *period* T, if it obeys $f(t) = f(t + T)$ for all values of t. Here we assume that the variable t represents time, which is relevant for spin dynamics calculations and in the acquisition of an experimental NMR time-domain

signal. The period T is associated with a *modulation frequency* ω_{mod}, which is inversely proportional to T:

$$\omega_{mod} = 2\pi/T \qquad [23]$$

Since T is given in units of seconds, ω_{mod} is an *angular frequency* given in rads per second. A frequency ν (Hz) is related to the corresponding angular frequency ω by

$$\omega = 2\pi\nu \qquad [24]$$

A periodic function may be expanded in a *Fourier series*

$$f(t) = \sum_{k=-M/2}^{M/2} f^{(k)} \exp\{ik\omega_{mod}t\} \qquad [25]$$

where the time-*in*dependent coefficients $f^{(k)}$ are called *Fourier components* (or Fourier coefficients). Equation [25] shows that $f(t)$ may be expressed as a sum over $M + 1$ Fourier components, each weighted by a complex exponential function involving a harmonic of ω_{mod}. The number of Fourier components required to reproduce the function f depends on the nature of its time dependence. In general, the more complicated dependence on time, the larger the number M. The value of M may sometimes extend to infinity. The Fourier components of a periodic function f may be calculated from the relationship

$$f^{(k)} = \frac{1}{T}\int_0^T dt\, f(t)\exp\{-ik\omega_{mod}t\};$$

$$k = -\frac{M}{2}, -\frac{M}{2}+1, \ldots, \frac{M}{2} \qquad [26]$$

In the theoretical formalism outlined in later sections, we will encounter *complex exponentials* of *periodic functions*, such as $g(t) = \exp\{if(t)\}$. Such exponential functions are also periodic, that is, $\exp\{if(t + T)\} = \exp\{if(t)\}$, and may consequently be expanded in a Fourier series, similar to Eq. [25]:

$$\exp\{if(t)\} = \sum_{k=-\infty}^{\infty} g^{(k)} \exp\{ik\omega_{mod}t\} \qquad [27]$$

Note, however, that even in the case of a finite number of Fourier components in Eq. [25], the Fourier series of $g(t)$ generally comprise an *infinite* number of Fourier components $g^{(k)}$.

Fourier Transforms. The Fourier transform (FT) is used extensively in the processing of NMR experiments: it converts an NMR time-domain signal $s(t)$ (amplitude as a function of time) into a frequency-domain spectrum $S(\omega)$ (amplitude as a function of frequency). The actual conversion is defined mathematically as an integration of the product $s(t)\exp\{-i\omega t\}$ over *all* time points t

$$S(\omega) = (2\pi)^{-1}\int_{-\infty}^{\infty} dt\, S(t)\exp\{-i\omega t\} \qquad [28]$$

A physical interpretation of the Fourier transform procedure may be found in Ref. (6). This operation is also invertible; the *inverse* Fourier transform (IFT) is defined as

$$s(t) = \int_{-\infty}^{\infty} d\omega\, S(\omega)\exp\{i\omega t\} \qquad [29]$$

It converts the frequency-domain spectrum $S(\omega)$ into the time-domain signal $s(t)$ by an integration of the product $S(\omega)\exp\{i\omega t\}$ over all frequencies ω. The interconversion between $s(t)$ and $S(\omega)$ by the Fourier transform and inverse Fourier transform operations is illustrated in Fig. 2 for the case of a simple NMR signal.

Discrete Fourier Series and Fourier Transforms. In practice, the experimentally acquired NMR time-domain signal is not continuous, but corresponds to a set of q discrete time points t_j and amplitudes $s(t_j)$: $\{t_j, s(t_j)\}$. All information known about the function $s(t)$ is contained in its q discrete values. A discretely sampled time signal is illustrated in Fig. 3. For practical reasons q is assumed to be *even.* The signal is sampled over an *acquisition interval* τ_{acq} at the equally spaced time points

$$t_j = j\tau_{acq}/q, \quad j = 0, 1, 2, \ldots, q-1 \qquad [30]$$

The duration between two time points t_j and t_{j+1} is usually called the *dwell time* (note, however, that it is a time *interval*) and may be calculated from either of the two following relationships:

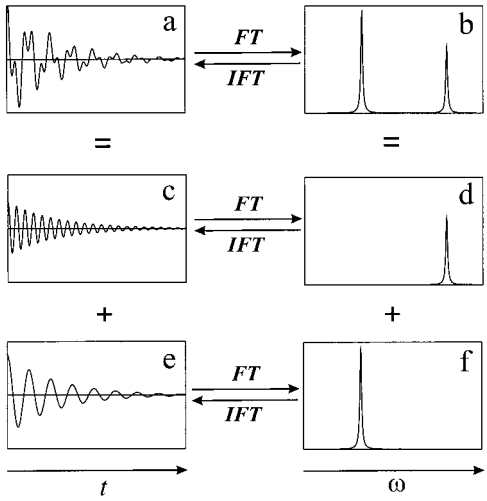

Figure 2 (a) The NMR time-domain signal is converted into (b) the frequency-domain spectrum by a Fourier transform (FT). The reverse transformation is effected by an inverse Fourier transform (IFT). In this case, the time-domain signal is a sum of two components, shown in (c) and (e), respectively. The corresponding spectra of the signals are shown in (d) and (f), respectively. Note that (c) the component with the higher oscillation frequency corresponds to (d) the peak at the higher frequency in the spectrum. Generally, the NMR signals are complex, but for simplicity, we have only displayed their real parts.

$$\tau_{\text{dwell}} = \tau_{\text{acq}}/q \qquad [31]$$

$$= 2\pi/\omega_{\text{samp}} \qquad [32]$$

where the sampling frequency ω_{samp} corresponds to the span of spectral frequencies (see Fig. 3).

The spectrum is obtained by a discrete Fourier transformation procedure (discussed below) and comprises the same number of points as does the time-domain signal. It corresponds to a set of frequency-amplitude pairs $\{\omega_k, a_k\}$. The expression for the amplitudes a_k are defined below, and the spectral coordinates are displaced around $\omega = 0$ and range from the negative frequency $-\omega_{\text{samp}}/2 + \omega_{\text{res}}$ to the positive frequency $-\omega_{\text{samp}}/2$. The qth frequency coordinate is (rad s^{-1}) given by

$$\omega_k = k\omega_{\text{res}}; \quad k = -\frac{q}{2} + 1, -\frac{q}{2} + 2, \ldots, \frac{q}{2} \qquad [33]$$

The frequency-domain resolution ω_{res} corresponds to the separation between two neighboring spectral coordinates: $\omega_{\text{res}} = \omega_{k+1} - \omega_k$. It may be calculated by dividing the spectral range ω_{samp} by the number of points q

$$\omega_{\text{res}} = \omega_{\text{samp}}/q \qquad [34]$$

or, alternatively, from the inverse of the acquisition interval

$$\omega_{\text{res}} = 2\pi/\tau_{\text{acq}} \qquad [35]$$

Note that ω_{res} has the same role in the frequency domain as the "dwell time" (τ_{dwell}) has in the time domain. The two entities are calculated from τ_{acq} and ω_{samp} using closely related expressions: Eq. [31] is

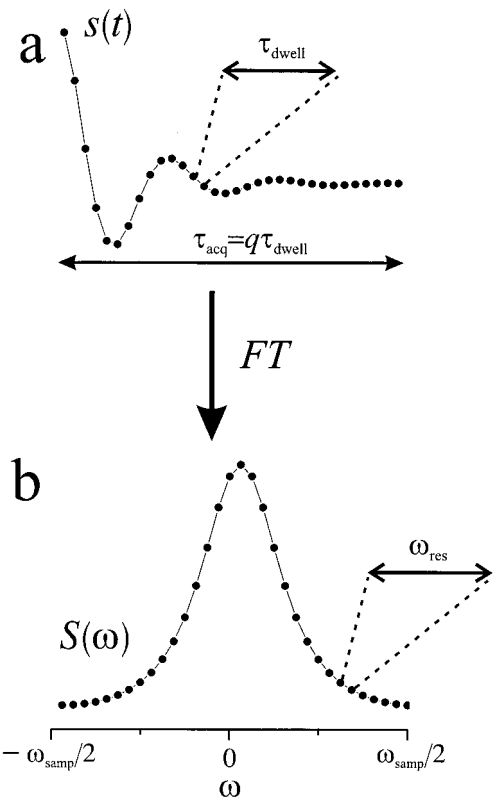

Figure 3 The relationship between parameters used when acquiring an NMR time-domain signal. (a) The signal is acquired at q discrete time points (in the present case, q = 32) with a duration τ_{dwell} between them. This results in a total time span τ_{acq}, called the acquisition interval. (b) Subsequent discrete Fourier transformation results in the NMR frequency-domain spectrum, consisting of q frequency–amplitude pairs. This extends over the frequency range ω_{samp}, which is inversely proportional to τ_{dwell} (Eq. [32]). The frequencies are spaced evenly in steps of the frequency resolution ω_{res}, ranging from the most negative frequency (left side of spectrum) $\omega = -\omega_{\text{samp}}/2 + \omega_{\text{res}}$ to the most positive value $\omega = \omega_{\text{samp}}/2$ (right side of spectrum). The frequency resolution is inversely proportional to the signal acquisition interval τ_{acq} (Eq. [35]). The lines between the points are only for visualization purposes and have no physical significance.

analogous to Eq. [34], whereas Eq. [32] is analogous to Eq. [35].

From Eq. [35] it follows that the longer the experimental acquisition interval, the finer the spectral resolution. Note that the convention used here for the spectral range ω_{samp} includes the positive frequency $\omega = +\omega_{\text{samp}}/2$ but *not* the corresponding negative value $\omega = -\omega_{\text{samp}}/2$. In fact, the amplitudes at the extreme positive and negative coordinates (i.e., $a_{-q/2}$ and $a_{q/2}$) are, by definition, *equal.* This follows from the properties of the Fourier transform of discrete data sets and is discussed in detail in Ref. (30). However, in order to keep the same number of points (q) in both the time and frequency domains, our convention is simply to drop the most negative frequency coordinate and use a slightly asymmetrical spectral range. This has negligible consequences in practice, as long as the frequency resolution ω_{res} is fine enough.

We point out that $s(t)$ is generally *not* periodic in time. However, functions that are sampled as discrete points t_j may always be expressed as a Fourier series according to Eq. [25]. References (4) and (30) explain the reasons for this property of discrete functions in more detail.

The corresponding set of Fourier components $\{a_k\}$ are obtained by a *discrete* Fourier transformation (*30*) of the set $\{s(t_j)\}$ as follows:

$$a_k = q^{-1} \sum_{j=0}^{q-1} s(t_j) \exp\{-i2\pi jk/q\};$$

$$k = -\frac{q}{2} + 1, -\frac{q}{2} + 2, \ldots, \frac{q}{2} \qquad [36]$$

The Fourier component a_k corresponds to the spectral *amplitude* at the frequency coordinate ω_k. Note that in Eq. [36] the index j runs over all integers $0 \leq j \leq q - 1$ whereas the index k takes integer values in the range $-(q/2) + 1 \leq k \leq q/2$.

As in the case of continuous functions, a discrete *inverse* Fourier transform is defined to produce $s(t_j)$ from the set of spectral amplitudes $\{a_k\}$ as follows:

$$s(t_j) = \sum_{k=-q/2+1}^{q/2} a_k \exp\{i2\pi jk/q\} \qquad [37]$$

We stress that we used *angular frequencies* for the spectral coordinates in this section. If desired, these may be converted into Hertz using Eq. [24].

Euler Angles and Rotation Operators

A counterclockwise rotation around an axis is defined as positive and a clockwise rotation as negative. The operator for a rotation by an angle θ around an axis $\vec{\mathbf{n}}$ is denoted $\hat{\mathbf{R}}_n(\theta)$ and defined as (*28, 29*)

$$\hat{\mathbf{R}}_n(\theta) = \exp\{-i\theta\vec{\hat{\mathbf{I}}} \cdot \vec{\mathbf{n}}\} \qquad [38]$$

where $\vec{\hat{\mathbf{I}}}$ is the total angular momentum operator.

A rotation of any 3-dimensional object can be specified by a sequence of three consecutive single-axis rotations and may, therefore, be parameterized by three axes and three corresponding angles. Here we make use of *passive* rotations, which are transformations of the coordinate systems rather than the objects themselves (*4, 28, 29*). The transformation of the coordinate system F with basis vectors $\{\vec{\mathbf{x}}_F, \vec{\mathbf{y}}_F, \vec{\mathbf{z}}_F\}$ into the system $F' = \{\vec{\mathbf{x}}_{F'}, \vec{\mathbf{y}}_{F'}, \vec{\mathbf{z}}_{F'}\}$ may be effected by the following sequence of rotations:

$$\hat{\mathbf{R}}(\alpha_{FF'}, \beta_{FF'}, \gamma_{FF'}) = \hat{\mathbf{R}}_{z_{F'}}(\gamma_{FF'})\hat{\mathbf{R}}_{y_G}(\beta_{FF'})\hat{\mathbf{R}}_{z_F}(\alpha_{FF'}) \qquad [39]$$

Equation [39] may be interpreted as follows: first the coordinate system is rotated around its $\vec{\mathbf{z}}_F$ axis by an angle $\alpha_{FF'}$. Then it is rotated around the y axis (here denoted $\vec{\mathbf{y}}_G$) of the *new* system by an angle $\beta_{FF'}$, followed by a rotation around the z axis of the "final" coordinate system F' by an angle $\gamma_{FF'}$. The rotation is therefore parameterized by a triplet of Euler angles [using the convention given on p. 21–22 of Ref. (28)]

$$\Omega_{FF'} = \{\alpha_{FF'}, \beta_{FF'}, \gamma_{FF'}\} \qquad [40]$$

where the angles take the values $\{0 \leq \alpha_{FF'} < 2\pi, 0 \leq \beta_{FF'} \leq \pi, 0 \leq \gamma_{FF'} < 2\pi\}$. Note that the subscripts FF' specify a transformation *from* system F *to* system F' (although intermediate systems are involved in each single-axis rotation). However, it may be shown (*28*) that the same transformation can be carried out by employing rotations solely around the axes of the original coordinate system F, if the *order* of rotations is *reversed:*

$$\hat{\mathbf{R}}(\alpha_{FF'}, \beta_{FF'}, \gamma_{FF'}) = \hat{\mathbf{R}}_{z_F}(\alpha_{FF'})\hat{\mathbf{R}}_{y_F}(\beta_{FF'})\hat{\mathbf{R}}_{z_F}(\gamma_{FF'}) \qquad [41]$$

Only two Euler angles are needed for specifying transformations of objects being symmetric around one axis, such as vectors. Equation [41] then reduces to a rotation by the angle $\beta_{FF'}$ around the y_F axis, followed by a rotation by the angle $\alpha_{FF'}$ around the z_F axis. This is illustrated in Fig. 4. In this case, the following relationship holds between the Euler angles $\{\alpha, \beta\}$ and the polar angles $\{\phi, \theta\}$:

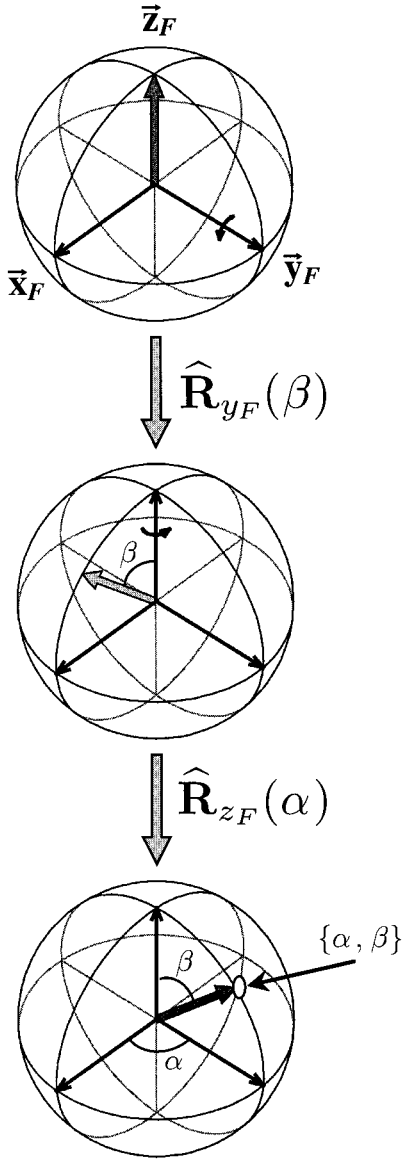

Figure 4 The orientation of an object that has a symmetry axis (e.g., a vector) may be parameterized by the two Euler angles $\{\alpha, \beta\}$, or equivalently, by the two polar angles $\{\theta, \phi\}$. Assume that the vector is aligned along the z_F axis of the coordinate system F (whose axes are labeled in the figure). According to Eq. [41], the vector may be rotated to the orientation $\{\alpha, \beta\}$ [indicated by the circle on the surface of the sphere shown in (c)] by a sequence of three rotations: first, by the angle γ around the z_F axis; second, by the angle β around the y_F axis; and third, by the angle α around the z_F axis. However, as a rotation around a symmetry axis leaves the vector unaffected, the first transformation around the z_F axis does not cause any net rotation. The second and third rotations give an orientation that in this case corresponds to the orientation $\{\alpha, \beta\} = \{\pi/2, \pi/4\}$, or in terms of polar angles, $\{\theta, \phi\} = \{\pi/4, \pi/2\}$.

$$\alpha \equiv \phi \qquad [42]$$

$$\beta \equiv \theta \qquad [43]$$

As discussed in a following publication, this relationship is useful for visualizing the orientational dependence of NMR interactions, especially when calculating powder averages.

In quantum mechanics, Eq. [41] is presented in terms of the *Wigner rotation operator* (*28*, *29*).

$$\hat{\mathbf{D}}(\alpha_{FF'}, \beta_{FF'}, \gamma_{FF'}) = \exp\{-i\alpha_{FF'}\hat{\mathbf{I}}_z\}\exp\{-i\beta_{FF'}\hat{\mathbf{I}}_y\}\exp\{-i\gamma_{FF'}\hat{\mathbf{I}}_z\} \qquad [44]$$

where we used the shorthand notation $x = x_F$, $y = y_F$, and $z = z_F$. The rotation operators are usually represented in a basis composed of a set of $2l + 1$ simultaneous eigenstates $\{|lm\rangle\}$ of the operator for the square of the total angular momentum $\hat{\mathbf{I}}^2$ and the operator $\hat{\mathbf{I}}_z$ (*28*, *29*):

$$\hat{\mathbf{I}}^2|lm\rangle = l(l+1)|lm\rangle \qquad [45]$$

$$\hat{\mathbf{I}}_z|lm\rangle = m|lm\rangle; \quad m = -l, -l+1, \ldots, l \qquad [46]$$

The "eigenequations" involve the quantum number l for the *total* angular momentum and its component m along the z direction (*28*, *29*). The matrix elements $D^l_{m'm}$ of the lth rank rotation operator are then given by

$$D^l_{m'm}(\Omega_{FF'}) \equiv \langle lm'|\hat{\mathbf{D}}(\Omega_{FF'})|lm\rangle = \langle lm'|\exp\{-i\alpha_{FF'}\hat{\mathbf{I}}_z\}\exp\{-i\beta_{FF'}\hat{\mathbf{I}}_y\} \times \exp\{-i\gamma_{FF'}\hat{\mathbf{I}}_z\}|lm\rangle \qquad [47]$$

where m and m' may take all integer values between $-l$ and l, giving a total of $(2l + 1) \times (2l + 1)$ such Wigner elements. It is convenient to define a *reduced Wigner element* (*28*, *29*) by

$$d^l_{m'm}(\beta_{FF'}) \equiv \langle lm'|\exp\{-i\beta_{FF'}\hat{\mathbf{I}}_y\}|lm\rangle \qquad [48]$$

and express $D^l_{m'm}(\Omega_{FF'})$ as

$$D^l_{m'm}(\Omega_{FF'}) = \exp\{-im'\alpha_{FF'}\}d^l_{m'm}(\beta_{FF'})\exp\{-im\gamma_{FF'}\} \qquad [49]$$

The reduced Wigner elements are real-valued functions of β. Explicit expressions for $d^1_{m'm}$ and $d^2_{m'm}$ are given in Table 1.

Table I Reduced Wigner Functions

$d^1_{m'm}(\beta)$

$m'\backslash m$	1	0	−1
1	$\frac{1}{2}(1+\cos\beta)$	$-\frac{1}{\sqrt{2}}\sin\beta$	$\frac{1}{2}(1-\cos\beta)$
0	$\frac{1}{\sqrt{2}}\sin\beta$	$\cos\beta$	$-\frac{1}{\sqrt{2}}\sin\beta$
−1	$\frac{1}{2}(1-\cos\beta)$	$\frac{1}{\sqrt{2}}\sin\beta$	$\frac{1}{2}(1+\cos\beta)$

$d^2_{m'm}(\beta)$

$m'\backslash m$	2	1	0	−1	−2
2	$\frac{1}{4}(1+\cos\beta)^2$	$-\frac{1}{2}\sin\beta\,(1+\cos\beta)$	$\sqrt{\frac{3}{8}}\sin^2\beta$	$-\frac{1}{2}\sin\beta\,(1-\cos\beta)$	$\frac{1}{4}(1-\cos\beta)^2$
1	$\frac{1}{2}\sin\beta\,(1+\cos\beta)$	$\frac{1}{2}(2\cos^2\beta+\cos\beta-1)$	$-\sqrt{\frac{3}{8}}\sin 2\beta$	$\frac{1}{2}(2\cos^2\beta-\cos\beta-1)$	$-\frac{1}{2}\sin\beta\,(1-\cos\beta)$
0	$\sqrt{\frac{3}{8}}\sin^2\beta$	$\sqrt{\frac{3}{8}}\sin 2\beta$	$\frac{1}{2}(3\cos^2\beta-1)$	$-\sqrt{\frac{3}{8}}\sin 2\beta$	$\sqrt{\frac{3}{8}}\sin^2\beta$
−1	$\frac{1}{2}\sin\beta\,(1-\cos\beta)$	$-\frac{1}{2}(2\cos^2\beta-\cos\beta-1)$	$\sqrt{\frac{3}{8}}\sin 2\beta$	$\frac{1}{2}(2\cos^2\beta+\cos\beta-1)$	$-\frac{1}{2}\sin\beta\,(1+\cos\beta)$
−2	$\frac{1}{4}(1-\cos\beta)^2$	$\frac{1}{2}\sin\beta\,(1-\cos\beta)$	$\sqrt{\frac{3}{8}}\sin^2\beta$	$\frac{1}{2}\sin\beta\,(1+\cos\beta)$	$\frac{1}{4}(1+\cos\beta)^2$

Irreducible Spherical Tensors

Many objects have properties that depend on their orientation with respect to measurements or certain manipulations. For example, a piece of wood or meat has fibers in certain directions, which makes it more difficult to cut across the direction of the fibers than parallel to them. This type of "anisotropic behavior" is closely related to the symmetry of the object with respect to the operation performed upon it.

"Anisotropic" objects are conveniently described in terms of irreducible spherical tensors. An irreducible spherical tensor of rank l, expressed in frame F, is composed of $2l + 1$ elements,

$$[\vec{\vec{\mathbf{A}}}^{(l)}]^F = ([A_{ll}]^F, [A_{ll-1}]^F, \ldots, [A_{l-l}]^F) \qquad [50]$$

with the mth component denoted $[A_{lm}]^F$ and in general represented by a complex number [Fig. 5(a)]. Note that the *number* of components of the irreducible spherical tensor depends on its rank. Components with opposite signs of the index m are related through

$$[A_{lm}]^F = (-1)^m [A_{l-m}]^F* \qquad [51]$$

where the asterisk denotes complex conjugation. Each component corresponds to the projection of the tensor onto a certain basis function (*4, 28, 29*); to define an lth rank tensor, $2l + 1$ basis functions are required. For example, consider a 3-dimensional vector represented in a Cartesian coordinate system $\vec{\mathbf{v}} = (v_x, v_y, v_z)$. Such a vector corresponds to a first-rank ($l = 1$) irreducible spherical tensor. Consequently, three basis "functions" are necessary to define the vector: in the present case, those are the three Cartesian orthogonal unit vectors, and each vector component v_j is given by the projection of $\vec{\mathbf{v}}$ onto the corresponding unit vector. For example, the component v_z is calculated as the scalar product of $\vec{\mathbf{v}}$ and $\vec{\mathbf{z}}$: $v_z = \vec{\mathbf{v}} \cdot \vec{\mathbf{z}}$.

The irreducible spherical tensor is *defined* by its response to rotations of the coordinate system, which

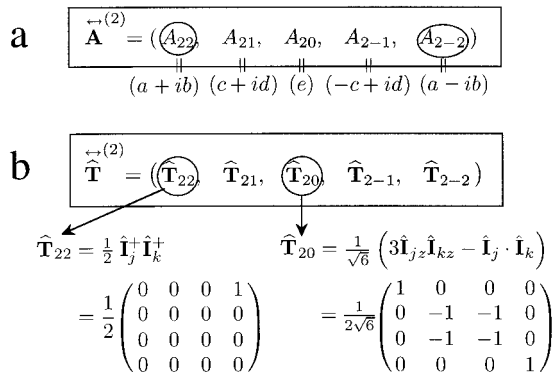

Figure 5 (a) A second rank ($l = 2$) irreducible spherical tensor has five components A_{lm}. Each of these is in a general reference frame represented by a *complex number*, except for A_{l0} which is real. The components A_{lm} and A_{l-m} are related through Eq. [51]. (b) The components of a second rank irreducible spherical tensor *operator*. The components $\hat{\mathbf{T}}_{lm}$ correspond to spin *operators*, represented as *matrices*. This example assumed operators for two coupled spins-$\frac{1}{2}$.

is completely specified by its rank l. Two irreducible spherical tensors of the same rank respond similarly to rotations, but these responses are different from that of another irreducible spherical tensor of different rank. An lth rank irreducible spherical tensor is transformed from frame F to frame F' by multiplication with the Wigner rotation operator of the same rank, according to

$$[\overleftrightarrow{\mathbf{A}}^{(l)}]^{F'} = [\overleftrightarrow{\mathbf{A}}^{(l)}]^{F}\hat{\mathbf{D}}^{(l)}(\Omega_{FF'}) \qquad [52]$$

It follows that the mth component of the tensor in the "new" frame is related to the components of the "old" frame according to

$$[A_{lm}]^{F'} = \sum_{m'=-l}^{l} [A_{lm'}]^{F} D^{l}_{m'm}(\Omega_{FF'}) \qquad [53]$$

Hence, under rotations, the *values* of the individual components change but the *number* of *components* is fixed. For example, the vector $\vec{\mathbf{v}}$ is always completely specified by exactly three components. This is the same as stating that the rank of an irreducible spherical tensor is conserved upon rotation, in the same way as the *shape* of a rigid object remains unchanged when the object is rotated. An object that responds equally in all directions is said to be *isotropic*. It is, therefore, invariant to rotations and may be represented as a zeroth rank ($l = 0$) tensor (a "scalar"). As discussed below, Eqs. [52] and [53] are used extensively for transforming NMR interactions between various coordinate systems.

Equation [52] may be viewed as a vector–matrix multiplication: the irreducible spherical tensor represented in frame F' is obtained by multiplying a row vector of dimension $2l + 1$ with a matrix of dimension $(2l + 1) \times (2l + 1)$. This interpretation is conveniently exploited in computer programs, especially if several consecutive transformations are needed. For example, the transformations $F \rightarrow F' \rightarrow F''$ may be carried out through

$$[\overleftrightarrow{\mathbf{A}}^{(l)}]^{F''} = [\overleftrightarrow{\mathbf{A}}^{(l)}]^{F}\hat{\mathbf{D}}^{(l)}(\Omega_{FF'})\hat{\mathbf{D}}^{(l)}(\Omega_{F'F''}) \qquad [54]$$

Note carefully the ordering of the subscripts.

The *scalar product* (inner product) of two irreducible spherical tensors is used extensively when constructing Hamiltonians in NMR. It is defined by

$$[\overleftrightarrow{\mathbf{A}}^{(l)}_{J}]^{F} \cdot [\overleftrightarrow{\mathbf{A}}^{(l)}_{K}]^{F} = \sum_{m=-l}^{l} (-1)^{m} [A^{J}_{lm}]^{F} [A^{K}_{l-m}]^{F} \qquad [55]$$

Sometimes the components of the spherical tensors are not complex numbers but *operators* [Fig. 5(b)]. An irreducible spherical tensor operator of rank l is denoted $\overleftrightarrow{\hat{\mathbf{T}}}^{(l)}$. Each of its $2l + 1$ components may be represented as a matrix in some suitable basis set, and it has the following symmetry upon sign reversal of m (*28, 29*):

$$\hat{\mathbf{T}}_{lm} = (-1)^{m}\hat{\mathbf{T}}^{\dagger}_{l-m} \qquad [56]$$

NMR INTERACTIONS IN SOLID STATE

Overview

The *Zeeman* interaction, which is the coupling of the spin angular momentum to the static magnetic field $\vec{B}_0$, is characterized by the Larmor frequency

$$\omega_0 = -\gamma_I B_0 \qquad [57]$$

where γ_I is the *magnetogyric ratio* (*1–6*) of the spins and B_0 is the magnitude of the field. However, each spin in the sample senses a slightly different magnetic field ("local field") at its location, because of its very specific chemical environment. The spin interactions arising from these local fields may be classified into chemical shift and spin–spin interactions (*1–6*). The spin–spin interactions that reflect couplings between the spins may be categorized further into *homonuclear* couplings (involving spins of the same species, e.g., two ^{1}H spins) and *heteronuclear* couplings (involving spins of different species, e.g., a ^{1}H and a ^{13}C). Also, depending on the mechanism of the couplings, the spin–spin interactions may be divided into through-space dipole–dipole (henceforth referred to as *dipolar* interactions) and through-bond (scalar) interactions (henceforth referred to as J interactions). Quadrupolar nuclei, having spin number $I > 1/2$, are also affected by first- and second-order quadrupolar interactions (*33*).

NMR Interactions in Terms of Irreducible Spherical Tensors

An important feature of NMR interactions is their dependence on the *orientation* of the molecule relative to the direction of the static magnetic field, implying that the NMR spectrum of a specific nuclear site in a molecule depends on the molecular orientation. This will be discussed in detail in a following publication. The interactions may be separated into parts that are *anisotropic* (orientation dependent) and

Table 2 Construction of Spin Hamiltonians from Spatial and Spin Components of Various Interactions

Interaction	C^Λ	A^Λ_{00}	$\hat{\mathbf{T}}^\Lambda_{00}$	$\hat{\mathbf{H}}^{\text{iso}}_\Lambda$	$[A^\Lambda_{20}]^L$	$[\hat{\mathbf{T}}^\Lambda_{20}]^L$	$\hat{\mathbf{H}}^{\text{aniso}}_\Lambda$
Chemical shift (CS)	$-\gamma_I$	$-\sqrt{3}\,\delta^j_{\text{iso}}$	$-\frac{1}{\sqrt{3}}\,B_0\hat{\mathbf{I}}_{jz}$	$\delta^j_{\text{iso}}\omega_0\hat{\mathbf{I}}_{jz}$	δ^j_{CSA}	$\sqrt{\frac{2}{3}}\,B_0\hat{\mathbf{I}}_{jz}$	$\omega^j_{\text{CSA}}\sqrt{\frac{2}{3}}\,\hat{\mathbf{I}}_{jz}$
Homonuclear dipolar (D)	1	—	—	—	ω^{jk}_D	$\frac{1}{\sqrt{6}}\,(3\hat{\mathbf{I}}_{jz}\hat{\mathbf{I}}_{kz}-\hat{\mathbf{I}}_j\cdot\hat{\mathbf{I}}_k)$	$\omega^{jk}_D\frac{1}{\sqrt{6}}\,(3\hat{\mathbf{I}}_{jz}\hat{\mathbf{I}}_{kz}-\hat{\mathbf{I}}_j\cdot\hat{\mathbf{I}}_k)$
Heteronuclear dipolar (D)	1	—	—	—	ω^{IS}_D	$\sqrt{\frac{2}{3}}\,\hat{\mathbf{I}}_z\hat{\mathbf{S}}_z$	$\omega^{IS}_D\sqrt{\frac{2}{3}}\,\hat{\mathbf{I}}_z\hat{\mathbf{S}}_z$
Homonuclear (J)	1	$-2\pi\sqrt{3}\,J^{jk}_{\text{iso}}$	$-\frac{1}{\sqrt{3}}\,\hat{\mathbf{I}}_j\cdot\hat{\mathbf{I}}_k$	$2\pi J^{jk}_{\text{iso}}\hat{\mathbf{I}}_j\cdot\hat{\mathbf{I}}_k$	$\omega^{jk}_{J,\text{aniso}}$	$\frac{1}{\sqrt{6}}\,(3\hat{\mathbf{I}}_{jz}\hat{\mathbf{I}}_{kz}-\hat{\mathbf{I}}_j\cdot\hat{\mathbf{I}}_k)$	$\omega^{jk}_{J,\text{aniso}}\frac{1}{\sqrt{6}}\,(3\hat{\mathbf{I}}_{jz}\hat{\mathbf{I}}_{kz}-\hat{\mathbf{I}}_j\cdot\hat{\mathbf{I}}_k)$
Heteronuclear (J)	1	$-2\pi\sqrt{3}\,J^{IS}_{\text{iso}}$	$-\frac{1}{\sqrt{3}}\,\hat{\mathbf{I}}_z\hat{\mathbf{S}}_z$	$2\pi J^{IS}_{\text{iso}}\hat{\mathbf{I}}_z\hat{\mathbf{S}}_z$	$\omega^{IS}_{J,\text{aniso}}$	$\sqrt{\frac{2}{3}}\,\hat{\mathbf{I}}_z\hat{\mathbf{S}}_z$	$\omega^{IS}_{J,\text{aniso}}\sqrt{\frac{2}{3}}\,\hat{\mathbf{I}}_z\hat{\mathbf{S}}_z$
First-order quadrupolar (Q)	$\frac{1}{2I(2I-1)}$	—	—	—	$[Q^j_{20}]^L$	$\frac{1}{\sqrt{6}}\,(3\hat{\mathbf{I}}^2_{jz}-I(I+1))$	$\omega^j_Q\frac{1}{\sqrt{6}}\,(3\hat{\mathbf{I}}^2_{jz}-I(I+1))$

The spin interaction Hamiltonians may be constructed from Eq. [20] as the product of a constant C^Λ, the spatial part in the laboratory frame $[A^\Lambda_{l0}]^L$, and the spin part $[\hat{\mathbf{T}}^\Lambda_{l0}]^L$. (See the discussion in the text regarding the chemical shift Hamiltonian.) The contribution from the $l = 0$ part of interaction Λ is obtained by multiplying columns 2, 3, and 4 of the given row. The result is given in column 5 ($\hat{\mathbf{H}}^{\text{iso}}_\Lambda$). The contribution from the $l = 2$ part is obtained by multiplication of columns 2, 6, and 7, resulting in the expression given in column 8 ($\hat{\mathbf{H}}^{\text{aniso}}_\Lambda$). The tensor components $[A^\Lambda_{2m}]^P$ necessary for obtaining $[A^\Lambda_{20}]^L$ are listed in Table 3. The various parameters and constants have the following meaning: for spin species I, γ_I denotes the gyromagnetic ratio and I is the spin number (i.e., total spin angular momentum). The isotropic components A_{iso} (e.g. δ^J_{iso} and J^{IS}_{iso}) are defined as the mean value of the principal values of the spatial tensor:

$$A_{\text{iso}} = \frac{1}{3}\left([A_{xx}]^P + [A_{yy}]^P + [A_{zz}]^P\right).$$

For the first-order quadrupolar interaction, the quadrupolar frequency is defined as

$$\omega^j_Q = \frac{[Q^j_{20}]^L}{2I(2I-1)}$$

isotropic (orientation independent). As explained further below, the isotropic parts correspond to the average of the interaction over all orientations of the molecule. However, in the cases of through-space dipolar and first-order quadrupolar interactions, the isotropic parts are zero.

It is convenient to describe the responses of the NMR interactions to molecular rotations by means of irreducible spherical tensors: each NMR interaction may be represented by a zeroth rank ($l = 0$) or second rank ($l = 2$) irreducible spherical tensor. The second-order quadrupolar interaction is a special case. We will not consider it here, but refer to Ref. (33) for details about this interaction.

NMR interactions may be thought of as deriving from two parts: one is dependent on "molecular properties" and is henceforth referred to as the "spatial tensor." The lth rank part of this tensor is denoted $\overleftrightarrow{\mathbf{A}}^{(l)}_\Lambda$, and it may be represented as a set of $2l + 1$ complex numbers A^Λ_{lm} as depicted in Fig. 5(a). The other, referred to as the "spin part," involves an irreducible spherical tensor operator $\overleftrightarrow{\mathbf{T}}^{(l)}_\Lambda$, which depends on spin angular momentum. The elements $\vec{\mathbf{T}}^\Lambda_{lm}$ correspond to spin operators that themselves are represented by matrices [Fig. 5(b)]. Together these two parts couple together to form what we refer to as the NMR "interaction."

General Form of Spin Hamiltonian

The spin Hamiltonian representing the interaction Λ may be expressed as a sum of scalar products of irreducible spherical tensors, where each scalar product involves a spatial tensor and a spin tensor (*1–5*). The irreducible spherical tensors may be expressed in different frames of reference. Because the Hamiltonian is a scalar product, it is independent of the choice of frame of the tensors (as long as they are represented in the *same* frame). However, the laboratory frame (L) is the natural choice. It is defined such that its z axis coincides with the direction of the static magnetic field. The laboratory frame Hamiltonian of interaction Λ may be expressed (*1–5*) as

$$\hat{\mathbf{H}}_\Lambda = C^\Lambda \sum_{l=0,2} [\overleftrightarrow{\mathbf{A}}^{(l)}_\Lambda]^L \cdot [\overleftrightarrow{\hat{\mathbf{T}}}^{(l)}_\Lambda]^L \qquad [58]$$

Using Eq. [55], this may be written

$$\hat{\mathbf{H}}_\Lambda = C^\Lambda \sum_{l=0,2} \sum_{m=-l}^{l} (-1)^m [A^\Lambda_{lm}]^L \cdot [\hat{\mathbf{T}}^\Lambda_{l-m}]^L \quad [59]$$

where C^Λ is a constant characteristic of the interaction.

In high-field NMR (ignoring second-order quadrupolar interactions in the case of quadrupolar nuclei), one may show that the only significant parts of the Hamiltonian are those whose spin parts commute with the the operator for the z component of the total spin angular momentum $\hat{\mathbf{I}}_z$. The commuting tensor operator components are $\hat{\mathbf{T}}^\Lambda_{l0}$ (*1–5*). Equation [59] then simplifies to

$$\hat{\mathbf{H}}_\Lambda = C^\Lambda \{A^\Lambda_{00} \hat{\mathbf{T}}^\Lambda_{00} + [A^\Lambda_{20}]^L [\hat{\mathbf{T}}^\Lambda_{20}]^L\} \quad [60]$$

Note that because the zeroth rank tensors are invariant to rotations, it is not necessary to specify the particular choice of reference frame for these. Equation [60] furnishes a framework for constructing Hamiltonians of spin interactions. The caption of Table 2 demonstrates how this may be done in practice for the chemical shift, dipolar, J, and first-order quadrupolar Hamiltonians. All Hamiltonians are given in angular frequency units (rad s^{-1}), as can be verified from the interaction parameters listed in Table 2.

We emphasize that the high-field spin Hamiltonian is a product of two components of irreducible spherical tensors, which have to be of the *same* rank l. In most cases they may be directly interpreted as a "spatial part" (which reflects how the interaction changes when the molecule is rotated) and a spin part (which reflects how the interaction changes upon rotations of the spin polarizations). Take, for example, the anisotropic heteronuclear J-coupling Hamiltonian $\hat{\mathbf{H}}^{IS}_{J,\text{aniso}}$. It involves a component of the J tensor, which is second rank with respect to rotations of the molecule. The spin part ($\sqrt{2/3}\,\hat{\mathbf{I}}_z\hat{\mathbf{S}}_z$) is *second* rank with respect to a simultaneous rotation of *both* the I and S spin polarizations. However, it is *first* rank with respect to rotations of *either* the I *or* S spin polarizations alone.

The classification of spatial and spin parts of the Hamiltonian is usually straightforward but may in some cases be obscure. This is especially the case for the chemical shift interaction involving the coupling of spins to the external magnetic field ($\vec{B}_0$) through the chemical shift (CS) tensor $\overleftrightarrow{\delta}_{CS}$, which may be decomposed into parts with $l = 0$, 1, or 2. The relevant ones to NMR are either zeroth or second rank with respect to rotations of the molecule. Strictly speaking, the "spin parts" of the chemical shift interaction given in Table 2 are components of the *spin-field* tensor $\overleftrightarrow{\mathcal{F}}$. This is first rank with respect to rotations of the spin polarizations and *additionally* first rank with respect to rotations of the external magnetic field. The spin-field tensor may be of both zeroth and second rank with respect to simultaneously rotating the spins and the direction of the external magnetic field. This is the reason for the appearance of the factors $-(1/\sqrt{3})\,B_0\hat{\mathbf{I}}_z$ and $\sqrt{2/3}\,B_0\hat{\mathbf{I}}_z$ in Table 2. Because the magnetic field direction is never changed in conventional NMR experiments, it is often practical to combine C^{CS}, B_0, and the relevant component of $\overleftrightarrow{\delta}_{CS}$ together. Loosely, this will be referred to as a "chemical shift tensor in frequency units," denoted $\overleftrightarrow{\omega}^{(l)}_{CS}$. Starting from its definition as a product of a chemical shift tensor component and a spin-field component, the Hamiltonian of the isotropic chemical shift interaction of spin j may be rearranged as

$$\hat{\mathbf{H}}^j_{\text{CS,iso}} = -\gamma_I \delta^j_{00} \hat{\mathcal{F}}^j_{00} \quad [61]$$

$$= -\gamma_I (-\sqrt{3}\delta^j_{\text{iso}}) \left(-\frac{1}{\sqrt{3}} B_0 \hat{\mathbf{I}}_{jz}\right) \quad [62]$$

$$= \delta^j_{\text{iso}} \omega_0 \hat{\mathbf{I}}_{jz} \quad [63]$$

using the expressions from Table 2 and the definition of the Larmor frequency (Eq. [57]). Equation [63] is the "conventional" form of the chemical shift Hamiltonian usually found in the literature (*1–6*).

In summary, care has to be taken when forming spin Hamiltonians from irreducible spherical tensors. However, because the Hamiltonian is crucial when writing numerical simulation programs, it is beneficial to exploit the irreducible spherical tensor concept, because it provides a general framework for systematic construction of Hamiltonians, as well as for theoretical analyses of NMR experiments.

SPIN OPERATORS

Zeeman Basis

The tensor operator components $\hat{\mathbf{T}}^\Lambda_{l0}$ appearing in the expression of the Hamiltonian (Eq. [60]) are linear combinations of spin operators. In a numerical simulation program, the explicit matrix representations are needed for these operators. The relationship between the $\hat{\mathbf{T}}^\Lambda_{l0}$ and the spin product operators for various NMR interactions are given in Table 2. The operators are normally represented in the Zeeman basis, which is the eigenbasis of $\hat{\mathbf{I}}_z$. Here we outline how this basis may be constructed for a system of coupled spins-$\frac{1}{2}$.

The basis set for systems of quadrupolar nuclei ($I > 1/2$) is constructed analogously.

A single spin-$\frac{1}{2}$ has two states of well-defined spin angular momentum along the static field direction. They are called *Zeeman states*: $|\alpha\rangle$ denotes the state with the quantum number for total spin angular momentum $I = 1/2$ and z component $m = 1/2$, whereas $|\beta\rangle$ is the state with $I = 1/2$ and z component $m = -1/2$. The two Zeeman states are represented by the following column vectors,

$$|\alpha\rangle = \begin{pmatrix} 1 \\ 0 \end{pmatrix} \quad [64]$$

$$|\beta\rangle = \begin{pmatrix} 0 \\ 1 \end{pmatrix} \quad [65]$$

Coupled spin systems require larger dimensions of the vectors representing the basis states. The spin operators for a system of N_I interacting spins-$\frac{1}{2}$ may be represented in a *Zeeman product basis* (*2*, *3*, *6*, *34*), which is formed by taking direct products of the Zeeman states of the individual spins.

$$|m_1 m_2 \cdots m_{N_I}\rangle \equiv |m_1\rangle \otimes |m_2\rangle \otimes \cdots \otimes |m_{N_I}\rangle \quad [66]$$

where $\otimes$ represents the direct product operation (*3*, *6*, *34*) and $|m_j\rangle$ is either $|\alpha\rangle$ or $|\beta\rangle$. It follows from combinatorics that a system of N_I spins-$\frac{1}{2}$ has 2^{N_I} different product basis states.

For instance, two spins-$\frac{1}{2}$ have four Zeeman product states: $\{|\alpha\alpha\rangle, |\alpha\beta\rangle, |\beta\alpha\rangle, |\beta\beta\rangle\}$. Each of these is obtained as a 4-dimensional vector from a direct product operation: for example, state $|\beta\alpha\rangle$ is calculated as $|\beta\rangle \otimes |\alpha\rangle$. Note carefully that the *order* of the states in Eq. [66] is important; for example, state $|\alpha\beta\rangle$ is *different* from $|\beta\alpha\rangle$. The direct product calculation is carried out by multiplying *each element* $|\beta\rangle_j$ of the vector representation $|\beta\rangle$ by the *entire vector* $|\alpha\rangle$:

$$|\beta\alpha\rangle = |\beta\rangle \otimes |\alpha\rangle = \begin{pmatrix} |\beta\rangle_1 \cdot |\alpha\rangle \\ |\beta\rangle_2 \cdot |\alpha\rangle \end{pmatrix} \quad [67]$$

Using the explicit representations of Eqs. [64] and [65], the calculations are carried out according to

$$|\beta\alpha\rangle = \begin{pmatrix} 0 \\ 1 \end{pmatrix} \otimes \begin{pmatrix} 1 \\ 0 \end{pmatrix} = \begin{pmatrix} 0 \cdot \begin{pmatrix} 1 \\ 0 \end{pmatrix} \\ 1 \cdot \begin{pmatrix} 1 \\ 0 \end{pmatrix} \end{pmatrix} = \begin{pmatrix} 0 \\ 0 \\ 1 \\ 0 \end{pmatrix} \quad [68]$$

This process may be used recursively for constructing the Zeeman basis states for larger spin systems. For example, the three-spin product state $|\beta\beta\alpha\rangle$ is, according to Eq. [66], calculated as $|\beta\beta\alpha\rangle = |\beta\rangle \otimes |\beta\rangle \otimes |\alpha\rangle$. The direct product operation is associative, meaning that we may form the state $|\beta\beta\alpha\rangle$ by two consecutive products, as either $|\beta\beta\alpha\rangle = |\beta\rangle \otimes (|\beta\rangle \otimes |\alpha\rangle)$ or $|\beta\beta\alpha\rangle = (|\beta\rangle \otimes |\beta\rangle) \otimes |\alpha\rangle$. The former calculation may alternatively be interpreted as $|\beta\beta\alpha\rangle = |\beta\rangle \otimes |\beta\alpha\rangle$. This means we may use the already obtained representation of $|\beta\alpha\rangle$ in Eq. [68] and calculate $|\beta\beta\alpha\rangle$ from the direct product of a 2-dimensional vector (representing $|\beta\rangle$) with a 4-dimensional vector (representing $|\beta\alpha\rangle$). The result is the following 8-dimensional vector:

$$|\beta\beta\alpha\rangle = |\beta\rangle \otimes |\beta\alpha\rangle = \begin{pmatrix} 0 \\ 1 \end{pmatrix} \otimes \begin{pmatrix} 0 \\ 0 \\ 1 \\ 0 \end{pmatrix} = \begin{pmatrix} 0 \\ 0 \\ 0 \\ 0 \\ 0 \\ 0 \\ 1 \\ 0 \end{pmatrix} \quad [69]$$

The Zeeman product states form an orthonormal basis set:

$$\langle m'_1 m'_2 \cdots m'_{N_I} | m_1 m_2 \cdots m_{N_I} \rangle = \delta(m'_1, m_1) \cdot \delta(m'_2, m_2) \cdots \delta(m'_{N_I}, m_{N_I}) \quad [70]$$

Each Zeeman product state for a multiple-spin system is simultaneously an eigenstate of the operators $\hat{\mathbf{I}}_{jz}$ ($1 \leq j \leq N_I$) for the individual spins, as well as of the operator for the z component of the *total* spin angular momentum $\hat{\mathbf{I}}_z = \hat{\mathbf{I}}_{1z} + \hat{\mathbf{I}}_{2z} + \cdots + \hat{\mathbf{I}}_{N_I z}$.

$$\hat{\mathbf{I}}_{jz} |m_1 m_2 \cdots m_{N_I}\rangle = m_j |m_1 m_2 \cdots m_{N_I}\rangle \quad [71]$$

$$\hat{\mathbf{I}}_z |m_1 m_2 \cdots m_{N_I}\rangle = (m_1 + m_2 + \cdots + m_{N_I}) |m_1 m_2 \cdots m_{N_I}\rangle \quad [72]$$

Note that $\hat{\mathbf{I}}_{jz}$ only operates on spin j and that all other spins stay unaffected. In a multispin system the operator $\hat{\mathbf{I}}_\zeta$ represents the sum over all spins (within the system) having angular momentum component ζ (where ζ represents x, y, z, $+$, or $-$).

$$\hat{\mathbf{I}}_\zeta = \sum_{j=1}^{N_I} \hat{\mathbf{I}}_{j\zeta} \quad [73]$$

For example, in a four-spin system the angular momentum raising operator $\hat{\mathbf{I}}^+$ corresponds to $\hat{\mathbf{I}}^+ = \hat{\mathbf{I}}_1^+ + \hat{\mathbf{I}}_2^+ + \hat{\mathbf{I}}_3^+ + \hat{\mathbf{I}}_4^+$ and increases the z-angular momentum by one unit for all spins.

Matrix Representations of Spin Operators

The matrix elements of spin operators can be calculated in the Zeeman product basis using Eq. [71] and the following expressions for the matrix elements of the raising and lowering operators $\hat{\mathbf{I}}_j^{\pm}$ (i.e., $\hat{\mathbf{I}}_j^+$ *or* $\hat{\mathbf{I}}_j^-$) (*4, 5, 28, 29*):

$$\langle m_1 m_2 \cdots m_j' \cdots m_{N_I} | \hat{\mathbf{I}}_j^{\pm} | m_1 m_2 \cdots m_j \cdots m_{N_I} \rangle = \sqrt{I(I+1) - m_j(m_j \pm 1)}\,\delta(m_j', m_j \pm 1) \quad [74]$$

Together with the following relations

$$\hat{\mathbf{I}}_{jx} = \frac{1}{2}(\hat{\mathbf{I}}_j^+ + \hat{\mathbf{I}}_j^-) \quad [75]$$

$$\hat{\mathbf{I}}_{jy} = \frac{1}{2i}(\hat{\mathbf{I}}_j^+ - \hat{\mathbf{I}}_j^-) \quad [76]$$

this is sufficient to calculate the matrix representation of any spin operator. For example, for a single spin-$\frac{1}{2}$, from Eqs. [71] and [74] the following matrices are obtained (*2–6, 28, 29*):

$$\hat{\mathbf{I}}_z = \frac{1}{2}\begin{pmatrix} 1 & 0 \\ 0 & -1 \end{pmatrix} \quad [77]$$

$$\hat{\mathbf{I}}_x = \frac{1}{2}\begin{pmatrix} 0 & 1 \\ 1 & 0 \end{pmatrix} \quad [78]$$

$$\hat{\mathbf{I}}_y = \frac{1}{2i}\begin{pmatrix} 0 & 1 \\ -1 & 0 \end{pmatrix} \quad [79]$$

As an example of calculations of matrix elements we construct some of the elements of the operator $\hat{\mathbf{I}}_{1z}\hat{\mathbf{I}}_{3x}$, assuming a system of three coupled spins-$\frac{1}{2}$. This operator may be interpreted as as a *product* of operators: $\hat{\mathbf{I}}_{1z}\hat{\mathbf{I}}_{3x} \equiv \hat{\mathbf{I}}_{1z} \cdot \hat{1}_2 \cdot \hat{\mathbf{I}}_{3x}$. Here $\hat{1}$ represents the unity operator and the matrix representation for each operator is of dimension 8×8. The index of the unity operator has no significance other than for bookkeeping reasons: it signifies that "spin number two" is unaffected by the operator $\hat{\mathbf{I}}_{1z}\hat{\mathbf{I}}_{3x}$. For example, the matrix element $\langle \alpha\alpha\alpha | \hat{\mathbf{I}}_{1z}\hat{\mathbf{I}}_{3x} | \alpha\alpha\beta \rangle$ may be evaluated according to the following steps:

$$\begin{aligned}\langle \alpha\alpha\alpha | \hat{\mathbf{I}}_{1z}\hat{1}_2\hat{\mathbf{I}}_{3x} | \alpha\alpha\beta \rangle &= \langle \underline{\alpha}\alpha\alpha | \hat{\mathbf{I}}_{1z} | \underline{\alpha}\alpha\beta \rangle \langle \alpha\underline{\alpha}\alpha | \hat{1}_2 | \alpha\underline{\alpha}\beta \rangle \\ &\quad \times \langle \alpha\alpha\underline{\alpha} | \hat{\mathbf{I}}_{3x} | \alpha\alpha\underline{\beta} \rangle \\ &= \frac{1}{2} \cdot 1 \cdot \frac{1}{2} \langle \alpha\alpha\underline{\alpha} | \hat{\mathbf{I}}_3^+ + \hat{\mathbf{I}}_3^- | \alpha\alpha\underline{\beta} \rangle \\ &= \frac{1}{4} \langle \alpha\alpha\underline{\alpha} | \hat{\mathbf{I}}_3^+ \alpha\alpha\underline{\beta} \rangle \\ &= \frac{1}{4}\end{aligned}$$

where each underlined state indicates the "part" of the bracket that is *affected* by the given operator. Likewise, it may be shown that $\langle \beta\beta\beta | \hat{\mathbf{I}}_{1z}\hat{\mathbf{I}}_{3x} | \beta\beta\beta \rangle = 0$ and $\langle \beta\beta\alpha | \hat{\mathbf{I}}_{1z}\hat{\mathbf{I}}_{3x} | \beta\beta\beta \rangle = -1/4$.

It is clear that this approach to calculate the elements becomes very tedious for even moderately large spin systems, because each operator is represented by a matrix of $2^{N_I} \times 2^{N_I}$ dimensions. Instead, it is much easier to construct matrix representations using the direct product (*3, 6, 34*). The direct product of two matrices $\mathbf{A} \otimes \mathbf{B}$ is effected by multiplying *each element* of the first matrix (A_{jk}) by the *entire* matrix $\mathbf{B}$. In the case of spins-$\frac{1}{2}$, the operators are represented by 2×2 matrices, and the resulting direct product operators are of dimension 4×4.

By exploiting the direct product, the matrix representation of the operator $\hat{\mathbf{I}}_{1z}\hat{\mathbf{I}}_{3x}$ may be obtained without extensive calculations as $\hat{\mathbf{I}}_{1z}\hat{\mathbf{I}}_{3x} = \hat{\mathbf{I}}_z \otimes \hat{1} \otimes \hat{\mathbf{I}}_x$, where the operators on the right-hand side correspond to single spin-$\frac{1}{2}$ operators. In this case, the direct product calculation involves forming an 8×8 matrix from three 2×2 matrices. The explicit calculation is given in Fig. 6, and further details of the construction of spin operators by direct products may be found in Refs. (3, 6, 34). This "direct product calculation" is the method of choice for numerical implementations. Alternatively, another technique for fast evaluation of matrix elements is described in Ref. (13).

SPATIAL TENSORS IN DIFFERENT FRAMES

Here we discuss how the spatial tensors of the NMR interactions may be constructed and represented in various commonly used reference frames. We especially focus on calculating $[A_{20}^{\Lambda}]^L$ because it is needed for obtaining the spin Hamiltonian (Eq. [60]).

Principal Axis System

Each tensor has the simplest form in its *principal axis system* (PAS), denoted P. In this frame, the magni-

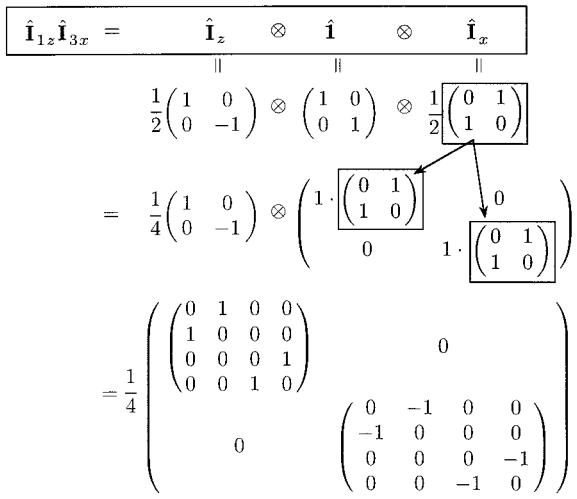

Figure 6 The recipe for constructing the matrix representation of the operator $\hat{\mathbf{I}}_{1z}\hat{\mathbf{I}}_{3x}$ for a system of three coupled spins-$\frac{1}{2}$, starting from three 2×2 matrices of each individual spin. This is performed using the direct product $\mathbf{A} \otimes \mathbf{B}$, evaluated by multiplying *each* element A_{mn} by the *entire matrix* $\mathbf{B}$. Here two consecutive direct products are required, which are evaluated from right to left as $\hat{\mathbf{I}}_{1z}\hat{\mathbf{I}}_{3x} = \hat{\mathbf{I}}_z \otimes (\hat{1} \otimes \hat{\mathbf{I}}_x)$. The first direct product creates a 4×4 matrix from two 2×2 matrices, and the second direct product operation gives the final matrix of dimension 8×8.

tude of the tensor may be characterized by three parameters, referred to as *principal values*, denoted $[A_{xx}]^P$, $[A_{yy}]^P$, and $[A_{zz}]^P$. For concreteness, we continue the discussion with the chemical shift tensor $\overleftrightarrow{\delta}_{CS}$, as an example.

In the deshielding convention (ppm), defined, for example, in Refs. (4, 6, 35), the chemical shift principal values are denoted $[\delta_{xx}]^P$, $[\delta_{yy}]^P$, and $[\delta_{zz}]^P$. From these it is convenient to introduce three new parameters,

$$\delta_{iso} = \frac{1}{3}\left([\delta_{xx}]^P + [\delta_{yy}]^P + [\delta_{zz}]^P\right) \qquad [80]$$

$$\delta_{aniso} = [\delta_{zz}]^P - \delta_{iso} \qquad [81]$$

$$\eta = \frac{[\delta_{yy}]^P - [\delta_{xx}]^P}{[\delta_{zz}]^P - \delta_{iso}} \qquad [82]$$

where δ_{iso} is the isotropic chemical shift, corresponding to the average of the shift tensor over all orientations. δ_{aniso} and η are called the *anisotropy* and the *asymmetry* parameter of the shift tensor, respectively. If the principal values are labeled such that

$$\left|[\delta_{zz}]^P - \delta_{iso}\right| \geq \left|[\delta_{xx}]^P - \delta_{iso}\right| \geq \left|[\delta_{yy}]^P - \delta_{iso}\right| \qquad [83]$$

the asymmetry parameter is in the range $0 \leq \eta \leq 1$ (*4, 5, 35*). Note that other definitions of η also exist in the literature. If $\eta = 0$, that is, if $[\delta_{yy}]^P = [\delta_{xx}]^P$, the tensor is referred to as being axially *symmetric* (*4, 5*). For all other values of η, the tensor is axially *asymmetric.*

The principal values of the chemical shift tensor may be extracted from the NMR spectrum. Due to rapid molecular reorientations, the isotropic chemical shift is the only directly observable parameter from spectra of isotropic liquids because the anisotropic parts average to zero. The spectrum corresponds to a single sharp peak, as shown in Fig. 7(a). From the spectrum of a static powder, on the other hand, the principal values may be read off directly as indicated in Fig. 7(b–d). These spectra are all for a constant shift anisotropy δ_{aniso} and different asymmetry parameters η. Note how the spectral line shape depends on the value of η. Also, a larger δ_{aniso} results in a broader spectrum. Using numerical simulation programs, one may determine chemical shift tensor parameters by iterative fitting of calculated and experimental spectra.

In the following we express the principal values in frequency units, as well as the isotropic and anisotropic shifts, by multiplying the various components with the Larmor frequency:

$$\omega_{iso} = \omega_0\delta_{iso} \qquad [84]$$

$$\omega_{aniso} = \omega_0\delta_{aniso} \qquad [85]$$

Note that often the principal values are given in shielding units σ, leading to sign reversal of the expressions for ω_{iso} and ω_{aniso} (*1, 4, 35*). From the equations above, the zeroth and second rank irreducible tensors describing the chemical shift interaction in its principal axis system may be expressed as

$$\overleftrightarrow{\omega}^{(0)}_{CS} = \omega^{CS}_{00} = -\sqrt{3}\,\omega_{iso} \qquad [86]$$

$$[\overleftrightarrow{\omega}^{(2)}_{CS}]^P = ([\omega^{CS}_{22}]^P, [\omega^{CS}_{21}]^P, [\omega^{CS}_{20}]^P, [\omega^{CS}_{2-1}]^P, [\omega^{CS}_{2-2}]^P)$$
$$= \omega_{aniso}\left(-\frac{1}{2}\eta,\, 0,\, \sqrt{\frac{3}{2}},\, 0,\, -\frac{1}{2}\eta\right) \qquad [87]$$

The rank two part $\overleftrightarrow{\omega}^{(2)}_{CS}$ is referred to as the *chemical shift anisotropy* (CSA) tensor. Note that this is a conflation of $\overleftrightarrow{\delta}^{(2)}_{CS}$ and B_0 and is strictly only a second rank tensor as long as the magnetic field direction is constant, as discussed earlier.

Definitions similar to those given above apply to *any* NMR interaction, provided that the relevant ten-

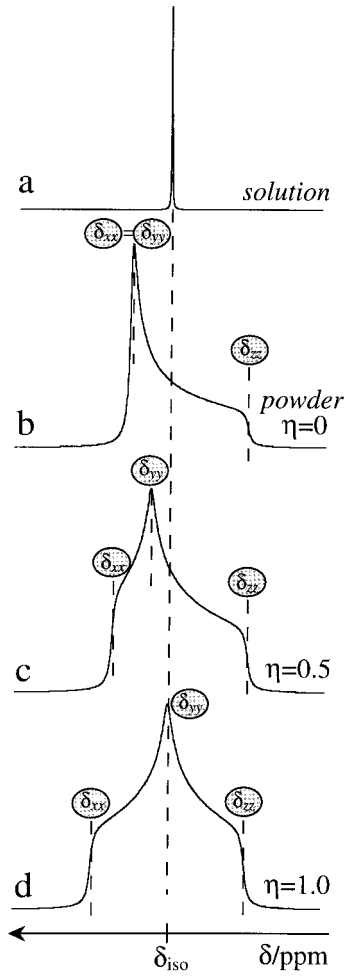

Figure 7 (a) The NMR spectrum of a chemical shift tensor from a sample in solution, displaying a sharp peak at the isotropic chemical shift δ_{iso}. (b–d) Spectra of a chemical shift tensor of a spin in a molecular fragment in a static powder. The spectra are for (b) one axially *symmetric* shift tensor and (c, d) two axially *asymmetric* tensors. The positions of the principal values of the tensor are shown in each case and they may be extracted from the shape of each powder pattern. (b–d) The chemical shift anisotropy parameter δ_{aniso} is the same in (b–d).

sor elements A^{Λ}_{lm} from Tables 2 and 3 are used. Thus, for a general anisotropy parameter A_{aniso} the tensor components are

$$[\overleftrightarrow{\mathbf{A}}^{(2)}]^P = A_{aniso}\left(-\frac{1}{2}\eta,\ 0,\ \sqrt{\frac{3}{2}},\ 0,\ -\frac{1}{2}\eta\right) \quad [88]$$

Molecular Frame

If one needs to consider several NMR interactions simultaneously in a calculation, it is common practice to transform the tensor representing each interaction into a common reference system that is fixed on the molecule; this *molecular frame* is denoted M and illustrated in Fig. 8(a). This procedure is convenient since all further transformations from the molecular frame are identical for all interactions. The Euler angles for transforming the second rank spatial tensor of interaction Λ from the principal axis system to its molecular frame are denoted Ω^{Λ}_{PM}. The transformation itself is carried out according to Eq. [52]:

$$[\overleftrightarrow{\mathbf{A}}^{(2)}_{\Lambda}]^M = [\overleftrightarrow{\mathbf{A}}^{(2)}_{\Lambda}]^P \hat{\mathbf{D}}^{(2)}(\Omega^{\Lambda}_{PM}) \quad [89]$$

The tensor components in the molecular frame $[A^{\Lambda}_{2m}]^M$ are related to those of the principal axis system through Eq. [53]:

$$[A^{\Lambda}_{2m}]^M = \sum_{m'=-2}^{2} [A^{\Lambda}_{2m'}]^P D^2_{m'm}(\Omega^{\Lambda}_{PM}) \quad [90]$$

Laboratory Frame

According to Eq. [60], only the $m = 0$ component of a tensor expressed in the laboratory frame, is required to construct the Hamiltonian. The following two subsections give the general expressions for the spatial tensor component A_{20} in the laboratory frame, which are appropriate for static and rotating solids, respectively.

Static Solid. Assuming a single interaction, the angles Ω^{Λ}_{PL} transform the second rank tensor from its principal axis system to the laboratory frame. In a powder containing randomly distributed crystallites, the angle Ω^{Λ}_{PL} is specific for each crystal orientation. The expression for $[A^{\Lambda}_{20}]^L$ in Eq. [60] is

$$[A^{\Lambda}_{20}]^L = \sum_{m=-2}^{2} [A^{\Lambda}_{2m}]^P D^2_{m0}(\Lambda^{\Lambda}_{PL}) \quad [91]$$

We may inspect the dependence of the tensor on each of the individual Euler angles $\{\alpha^{\Lambda}_{PL},\ \beta^{\Lambda}_{PL},\ \gamma^{\Lambda}_{PL}\}$ by using Eq. [49]

$$D^2_{m0}(\Omega^{\Lambda}_{PL}) = \exp\{-im\alpha^{\Lambda}_{PL}\} d^2_{m0}(\beta^{\Lambda}_{PL}) \exp\{-i0\gamma^{\Lambda}_{PL}\} \quad [92]$$

$$= d^2_{m0}(\beta^{\Lambda}_{PL}) \exp\{-im\alpha^{\Lambda}_{PL}\} \quad [93]$$

and rewriting Eq. [91] as

Table 3 Components A^{Λ}_{2m}, $-2 \le m \le 2$, of Second Rank Spatial Tensors in Their Principal Axis System

Interaction (Λ)	$[A^{\Lambda}_{20}]^P$	$[A^{\Lambda}_{2\pm1}]^P$	$[A^{\Lambda}_{2\pm2}]^P$
Chemical shift (CS)	$\sqrt{\frac{3}{2}}\,\delta^j_{\text{aniso}}$	0	$-\frac{1}{2}\,\eta\delta^j_{\text{aniso}}$
Homonuclear dipolar (D)	$\sqrt{6}\,b^{jk}$	0	0
Heteronuclear dipolar (D)	$\sqrt{6}\,b^{IS}$	0	0
Homonuclear J	$2\pi\ \sqrt{\frac{3}{2}}\,J^{jk}_{\text{aniso}}$	0	$-\frac{1}{2}\,\eta J^{jk}_{\text{aniso}}$
Heteronuclear J	$2\pi\ \sqrt{\frac{3}{2}}\,J^{IS}_{\text{aniso}}$	0	$-\frac{1}{2}\,\eta J^{IS}_{\text{aniso}}$
First-order quadrupolar (Q)	$\sqrt{\frac{3}{2}}\,\chi_Q$	0	$-\frac{1}{2}\,\eta\chi_Q$

The anisotropies A_{aniso} of the spatial tensors (e.g., δ_{aniso} and J^{jk}_{aniso}) are defined as

$$A_{\text{aniso}} = [A_{zz}]^P - A_{\text{iso}}$$

with A_{iso} given by

$$A_{\text{iso}} = \tfrac{1}{3}\,([A_{xx}]^P + [A_{yy}]^P + [A_{zz}]^P$$

The asymmetry parameter for each interaction is defined

$$\eta = [A_{yy}]^P - [A_{xx}]^P/([A_{zz}]^P - A_{\text{iso}})$$

The dipolar coupling constants b^{jk} and b^{IS} are defined

$$b_{jk} = \mu_0\gamma_I^2\hbar/(4\pi r^3_{jk}) \quad \text{and} \quad b^{IS} = \mu_0\gamma_I\gamma_S\hbar/(4\pi r^3_{jk})$$

with r_{jk} and r_{IS} being the distances between the two spins in the homonuclear and heteronuclear spin pair, respectively; $\mu_0 = 4\pi \cdot 10^7\text{NC}^{-2}\text{s}^2$ is the permeability of vacuum and $\hbar$ is Planck's constant ($h = 6.62608 \cdot 10^{-34}$ Js) divided by 2π. The quadrupolar tensor ($\overleftrightarrow{Q}^{(2)}$) is defined as the product of the electric field gradient tensor and the quadrupolar moment of the nucleus (eQ). With this definition, the magnitude of the anisotropy of the quadrupolar interaction is given by the quadrupolar coupling constant $\chi_Q = e^2qQ/\hbar$. The following units are employed for the anisotropies: χ_Q and b (rad s^{-1}), δ_{aniso} (ppm), and J_{aniso} (Hz).

$$[A^{\Lambda}_{20}]^L = \sum_{m=-2}^{2} [A^{\Lambda}_{2m}]^P d^2_{m0}(\beta^{\Lambda}_{PL})\exp\{-im\alpha^{\Lambda}_{PL}\} \qquad [94]$$

Equation [94] shows that there is *no* dependence on the Euler angle γ_{PL}, which has implications when simulating NMR responses from powders. In a following publication, such orientational considerations will be discussed in detail.

In the case of several interactions (Λ_1, Λ_2, Λ_3, . . .), it is useful to exploit transformations via the molecular frame. Assuming the sequence of transformations through the reference frames $P \rightarrow M \rightarrow L$ [see Fig. 8(a) for a physical interpretation of these transformations], the laboratory frame component $[A^{\Lambda}_{20}]^L$ is given by

$$[A^{\Lambda}_{20}]^L = \sum_{m,m'=-2}^{2} [A^{\Lambda}_{2m'}]^P D^2_{m'm}(\Omega^{\Lambda}_{PM})\, D^2_{m0}(\Omega_{ML}) \qquad [95]$$

In a powder, the angle Ω^{Λ}_{PM} is specific for each interaction but common to all crystallites in the sample, whereas the angle Ω_{ML} is the same for all interactions of each crystal orientation. Therefore, the tensor for each interaction (Λ_1, Λ_2, Λ_3, . . .) is usually first transformed to the molecular frame using Eq. [89]. The component $[A^{\Lambda}_{20}]^L$ is related to the tensor components in the molecular frame by

$$[A^{\Lambda}_{20}]^L = \sum_{m=-2}^{2} [A^{\Lambda}_{2m}]^M D^2_{m0}(\Omega_{ML}) \qquad [96]$$

$$= \sum_{m=-2}^{2} [A^{\Lambda}_{2m}]^M d^2_{m0}(\beta_{ML})\exp\{-im\alpha_{ML}\} \qquad [97]$$

where the last equality follows by using Eq. [49].

Rotating Solid. In the theoretical treatment of MAS experiments, it is convenient to define a reference frame R on the sample holder (rotor) such that the z axis of that "rotor frame" is along the sample rotation axis [Fig. 8(b)]. Assume that the sample is spun at the

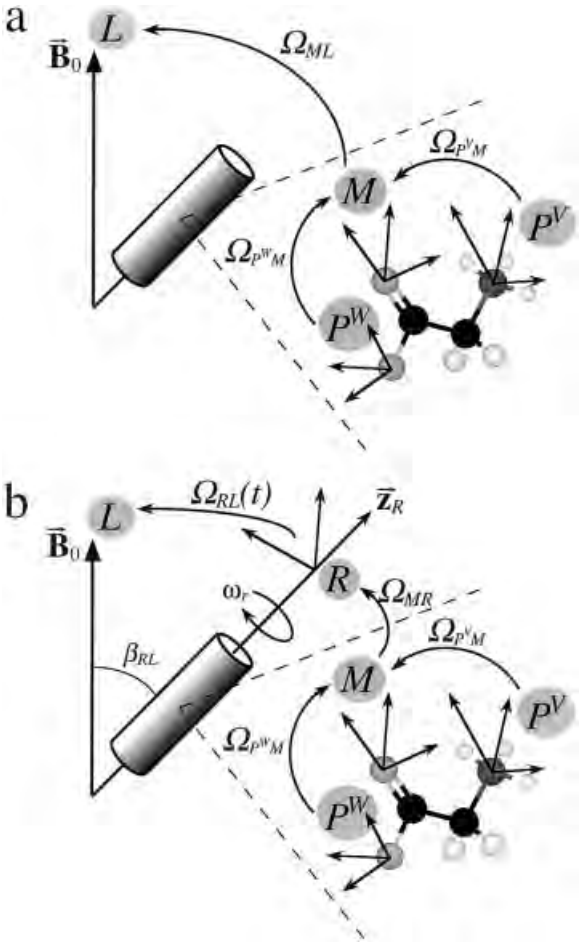

Figure 8 Visualization of different frames and transformations employed in solid-state NMR. Each principal axis system of two spatial tensors are shown (P^V, P^W). Each of these is related to the molecular frame M by the Euler angles Ω^V_{PM} and Ω^W_{PM}, respectively. (a) The transformations relevant for a calculation of a static sample. (b) Analogous transformations for a calculation of a rotating sample. The rotor frame R is chosen such that its z axis subtends the angle β_{RL} with the static field direction. For magic-angle spinning, $\beta_{RL} = \arctan\sqrt{2}$. The coordinate system M is related to the rotor frame by the angles Ω_{MR}, and the final transformation into the laboratory frame is given by the time-dependent angles $\Omega_{RL}(t) = \{-\omega_r t, \theta_m, 0\}$.

magic angle at a fixed angular frequency ω_r, associated with a rotational period

$$\tau_r = 2\pi/\omega_r \qquad [98]$$

corresponding to the time interval for the rotor to make a complete revolution. The sample rotation gives rise to *time-dependent* Euler transformation angles $\Omega_{RL}(t)$ relating the rotor frame R to the laboratory frame L. For MAS these are at a certain instant of time t given by

$$\Omega_{RL}(t) = \{\alpha_{RL}(t), \beta_{RL}, \gamma_{RL}\} = \{-\omega_r t, \theta_m, 0\} \qquad [99]$$

with the "magic angle" is given by $\theta_m = \arctan\sqrt{2}$. In the case of sample rotation off the magic angle, β_{RL} takes an arbitrary value.

For practical calculations of rotating samples, the transformation of a general second rank spatial tensor from an arbitrary molecular frame to the laboratory frame is performed by the following sequence of rotations [depicted in Fig. 8(b)]:

$$[\overleftrightarrow{\mathbf{A}}^{(2)}_\Lambda]^M \xrightarrow{\Omega_{MR}} [\overleftrightarrow{\mathbf{A}}^{(2)}_\Lambda]^R \xrightarrow{\Omega_{RL}} [\overleftrightarrow{\mathbf{A}}^{(2)}_\Lambda]^L \qquad [100]$$

Following the same calculations as in the static case, the tensor in the laboratory frame is expressed

$$[\overleftrightarrow{\mathbf{A}}^{(2)}_\Lambda]^L = [\overleftrightarrow{\mathbf{A}}^{(2)}_\Lambda]^M \hat{\mathbf{D}}^{(2)}(\Omega_{MR})\hat{\mathbf{D}}^{(2)}(\Omega_{RL}(t)) \qquad [101]$$

After carrying out the transformations and using Eq. [49], the component $[A^\Lambda_{20}]^L$ may be written

$$[A^\Lambda_{20}]^L = \sum_{m',m=-2}^{2} [A^\Lambda_{2m'}]^M D^2_{m'm}(\Omega_{MR}) d^2_{m0}(\theta_m)\exp\{im\omega_r t\} \qquad [102]$$

and identified with a time-dependent frequency $\omega_\Lambda(t) = [A^\Lambda_{20}]^L$. Inspection of Eq. [102] reveals that it is a Fourier series; it conforms to Eq. [25] with ω_{mod} given by ω_r,

$$\omega_\Lambda(t) = \sum_{m=-2}^{2} \underbrace{\sum_{m'=-2}^{2} [A^\Lambda_{2m'}]^M D^2_{m'm}(\Omega_{MR}) d^2_{m0}(\theta_m)}_{\omega^{(m)}_\Lambda} \times \exp\{im\omega_r t\} \qquad [103]$$

$$= \sum_{m=-2}^{2} \omega^{(m)}_\Lambda \exp\{im\omega_r t\} \qquad [104]$$

and the five Fourier components $\omega^{(m)}_\Lambda$ related to the tensor components $[A^\Lambda_{2m'}]^M$ according to

$$\omega^{(m)}_\Lambda = \sum_{m'=-2}^{2} [A^\Lambda_{2m'}]^M D^2_{m'm}(\Omega_{MR}) d^2_{m0}(\theta_m) \qquad [105]$$

The frequency $\omega_\Lambda(t)$ is a real number, and the Fourier components $\omega^{(m)}_\Lambda$ and $\omega^{(-m)}_\Lambda$ are related by

$$\omega_\Lambda^{(m)} = \{\omega_\Lambda^{(-m)}\}^* \qquad [106]$$

This relationship is useful, for example, to speed up numerical calculations, because it follows that only $\omega_\Lambda^{(m)}$ for $m \geq 0$ needs to be calculated explicitly by Eq. [105]. This limits the calculation to only three out of five components, because the remaining two may be obtained directly from Eq. [106]. Consequently, Eq. [104] may be written

$$\omega_\Lambda(t) = \omega_\Lambda^{(0)} + 2\sum_{m=1}^{2} \mathrm{Re}\{\omega_\Lambda^{(m)}\}\cos\{m\omega_r t\} - \mathrm{Im}\{\omega_\Lambda^{(m)}\}\sin\{m\omega_r t\} \qquad [107]$$

Equations [106] and [107] are proven in Appendix A.

Equation [104] shows how MAS induces a *time-periodic* modulation of the second rank spatial tensors. The value of $\omega_\Lambda(t_0)$ is equal to that following completion of a full rotational period: $\omega_\Lambda(t_0) = \omega_\Lambda(t_0 + \tau_r)$. This may be verified by inserting the two different time points into Eq. [104]. Using $\omega_r\tau_r = 2\pi$, the exponential factor may be expressed as $\exp\{im\omega_r(t_0 + \tau_r)\} = \exp\{im\omega_r t_0\}\exp\{2im\pi\} = \exp\{im\omega_r t_0\}$. This demonstrates that the spatial part of the Hamiltonian is periodic in time.

Rotating Frame

Although we have thus far stressed the laboratory frame as the "final" reference frame, in practice an additional transformation of the Hamiltonian is normally employed: one to the *rotating frame* (*1–6*). This involves *transforming* the *spin parts* of the Hamiltonian, and it must be distinguished from the rotor frame *R* of the previous section. Employing the rotating frame means observing the NMR experiment from a time-dependent coordinate system, where the transverse plane rotates around its *z* axis (which coincides with that of the laboratory frame) at a constant rate ω_{ref}, close to the Larmor frequency of the spins.

The resulting rotating frame spin Hamiltonian includes all interactions of the local magnetic fields, such as the chemical shifts and dipolar couplings, but excludes the Zeeman interaction. The rotating frame Hamiltonian may be obtained from the laboratory frame Hamiltonian after subtracting the term $\omega_{\mathrm{ref}}\hat{\mathbf{I}}_z$ from the latter. The explicit transformations are given in Refs. (2–6, 35).

NMR TIME-DOMAIN SIGNAL AND SPECTRUM

The remainder of the article discusses how the NMR signal in both the time and frequency domains is obtained as a result of the time evolution of the spin system. In this section a general formalism for calculating the time-domain signal under any experimental circumstance is outlined. The next section discusses concepts of dynamically homogeneous and inhomogeneous Hamiltonians. Next, the form of the NMR signal is derived for the case of a dynamically inhomogeneous Hamiltonian. Two specific classes of dynamically inhomogeneous problems are examined in more detail: experiments with a static sample and a rotating sample. Computer code for simulating NMR time-domain signals and frequency-domain spectra for these cases will be provided in the two following articles.

Density Operator

NMR experiments are normally performed on a very large *ensemble* of nuclear spin systems, where the spins may interact with each other within each system, but the various ensemble members (i.e., spin systems) are independent of each other. In such cases, the *density operator* formalism is applicable. This is a statistical approach, having the advantage that one obtains a density operator $\hat{\rho}$, representing the entire ensemble state, without the need to consider the state of each individual spin system in the very large ensemble. Further information about the density operator formalism may be found in Refs. (2–6, 29, 34).

The density operator is represented by the *density matrix* in a suitable basis set. For example, for an ensemble of isolated spins-$\frac{1}{2}$, the density matrix may in the Zeeman basis be written

$$\hat{\rho} = \begin{pmatrix} \langle\alpha|\hat{\rho}|\alpha\rangle & \langle\alpha|\hat{\rho}|\beta\rangle \\ \langle\beta|\hat{\rho}|\alpha\rangle & \langle\beta|\hat{\rho}|\beta\rangle \end{pmatrix} \qquad [108]$$

Each element of the density matrix represents the spin ensemble in various states: the diagonal elements correspond to fractional *populations* of the states, whereas the off-diagonal elements represent *coherences*. We refer to Refs. (2–6) for the exact meanings of these terms. In the case of isolated spins-$\frac{1}{2}$, the elements $\langle\alpha|\hat{\rho}|\alpha\rangle$ and $\langle\beta|\hat{\rho}|\beta\rangle$ give the fractional populations of the states $|\alpha\rangle$ and $|\beta\rangle$, respectively. If the magnitudes of these elements are *different* there is a net *longitudinal* spin polarization (and magnetization) along the static field direction. The two off-diagonal

elements $\langle\alpha|\hat{\rho}|\beta\rangle$ and $\langle\beta|\hat{\rho}|\alpha\rangle$ correspond to -1 and $+1$ quantum coherences (-1QC and $+1$QC), respectively. The presence of single-quantum coherences in the ensemble is equivalent to a net spin polarization (and magnetization) in the *transverse* plane of the rotating frame. The spin density operator may be expressed as a linear combination of spin operators of the system. Net longitudinal magnetization corresponds to a density operator proportional to $\hat{\mathbf{I}}_z$, whereas transverse magnetization corresponds to $\hat{\rho}$ being proportional to a combination of $\hat{\mathbf{I}}_x$ and $\hat{\mathbf{I}}_y$, or equivalently, a linear combination of $\hat{\mathbf{I}}^+$ and $\hat{\mathbf{I}}^-$. (See Eqs. [75] and [76] for the relationship between the various operators.)

The density operator of an ensemble of isolated spins-$\frac{1}{2}$ may be written using the Dirac formalism as

$$\hat{\rho} = \sum_{j,k=\alpha,\beta}^{\mathcal{N}} \langle j|\hat{\rho}|k\rangle \cdot |j\rangle\langle k| \qquad [109]$$

$$= \langle\alpha|\hat{\rho}|\alpha\rangle \cdot |\alpha\rangle\langle\alpha| + \langle\alpha|\hat{\rho}|\beta\rangle \cdot |\alpha\rangle\langle\beta| + \langle\beta|\hat{\rho}|\alpha\rangle \cdot |\beta\rangle\langle\alpha| + \langle\beta|\hat{\rho}|\beta\rangle \cdot |\beta\rangle\langle\beta| \qquad [110]$$

The explicit matrix representation of Eq. [110] corresponds to Eq. [108]. The operators $|\alpha\rangle\langle\beta|$ and $|\beta\rangle\langle\alpha|$ correspond to $+1$QC and -1QC, respectively. For example, it may be verified that the operator $|\beta\rangle\langle\alpha|$ corresponds to $\hat{\mathbf{I}}^-$ by letting it operate on each of the Zeeman basis states $|\alpha\rangle$ and $\langle\beta|$. We get

$$(|\beta\rangle\langle\alpha|) \cdot |\alpha\rangle = |\beta\rangle \cdot \langle\alpha|\alpha\rangle = |\beta\rangle$$

and

$$(|\beta\rangle\langle\alpha|) \cdot |\beta\rangle = |\beta\rangle \cdot \langle\alpha|\beta\rangle = 0$$

as expected from the operator $\hat{\mathbf{I}}^-$: it converts state $|\alpha\rangle$ into state $\langle\beta|$. Likewise, it may be demonstrated that $|\alpha\rangle\langle\beta| = \hat{\mathbf{I}}^+$.

In the general case of an ensemble consisting of multiple-spin systems, with the spin operators represented in an arbitrary basis spanned by $\mathcal{N}$ states $\{|1\rangle, |2\rangle, \ldots, |\mathcal{N}\rangle\}$, the density operator may formally be expressed in the Dirac formalism as the following sum:

$$\hat{\rho} = \sum_{j,k=1}^{\mathcal{N}} \langle j|\hat{\rho}|k\rangle \cdot |j\rangle\langle k| \qquad [111]$$

This expression may be derived by multiplying the density operator from both sides by the unity operator, $\hat{1}\hat{\rho}\hat{1}$, and then inserting the closure relation (*29*)

$$\sum_{j=1}^{\mathcal{N}} |j\rangle\langle j| = \hat{1} \qquad [112]$$

which states that the sum over all *projection operators* $|j\rangle\langle j|$ (*2–6, 29, 34*) equals the unity operator. Then we obtain the expression

$$\hat{\rho} = \sum_{j,k=1}^{\mathcal{N}} |j\rangle\langle j| \cdot \hat{\rho} \cdot |k\rangle\langle k| \qquad [113]$$

Equation [111] follows from interpreting the product $|j\rangle\langle j| \cdot \hat{\rho} \cdot |k\rangle\langle k|$ as $|j\rangle \cdot \langle j|\hat{\rho}|k\rangle \cdot \langle k|$ and then using that $\langle j|\hat{\rho}|k\rangle$ as a complex number that may be rearranged within the product. (Similar calculations were carried out in an earlier section.)

Note that the basis employed in Eq. [111] may *not necessarily* be the Zeeman product basis. Formally, the interpretation of the diagonal and off-diagonal elements in terms of populations and coherences is similar, regardless of the choice of basis. However, unless the Zeeman basis is employed, the *physical meanings* of the matrix elements (e.g., in terms of spin polarizations and magnetizations) *differ* from the usual interpretations. In the following, we will frequently express the density operator in the eigenbasis of the Hamiltonian, because this is well suited for describing spin dynamics (*10–13, 15, 17, 18*).

The starting point for any NMR experiment is the spin ensemble at thermal equilibrium in a strong magnetic field $\vec{\mathbf{B}}$. Over the ensemble, there is a net polarization pointing along the static magnetic field (i.e., a net longitudinal polarization). As pointed out earlier, this corresponds to a density operator being proportional to $\hat{\mathbf{I}}_z$ (*2–6, 34*),

$$\hat{\rho}_{\text{eq}} \propto (\hat{1} + \beta_I \hat{\mathbf{I}}_z) \qquad [114]$$

where β_I is the Boltzmann factor, given by

$$\beta_I = \frac{-\hbar\gamma_I B_0}{k_B T} \qquad [115]$$

Here T is the temperature (K) and $k_B = 1.381 \cdot 10^{-23}$ JK^{-1} is the Boltzmann constant. The unity operator and the Boltzmann factor will not affect any of the results in our treatment and will be dropped.

The thermal equilibrium density operator used in the following is then given by

$$\hat{\rho}_{\mathrm{eq}} = \hat{\mathbf{I}}_z \qquad [116]$$

Time Evolution of Density Operator

Assume the spin ensemble is initially at $t = t_a$ in a certain state represented by $\hat{\rho}(t_a)$ and that the total spin Hamiltonian (including the contributions from all interactions) does not commute with $\hat{\rho}(t_a)$. Then the Hamiltonian will cause a change of the spin ensemble state, which mathematically translates into a *change of the density operator;* it becomes *time dependent:*

$$\hat{\rho}(t_a) \xrightarrow{\hat{\mathbf{H}}} \hat{\rho}(t) \qquad [117]$$

The central question when dealing with quantum dynamics in NMR is, *given that we know the density operator at the time point t_a, how do we find its expression at a later time point t_b*? The solution to the problem is the operator $\hat{\mathbf{U}}(t_b, t_a)$, called the *propagator*, which transforms the density operator according to the following "sandwich formula" (*2–6, 29*):

$$\hat{\rho}(t_b) = \hat{\mathbf{U}}(t_b, t_a)\hat{\rho}(t_a)\hat{\mathbf{U}}(t_b, t_a)^{\dagger} \qquad [118]$$

Note that the time points are written such that *later* times appear to the *left*, for example, the propagator transforming $\hat{\rho}(t_a)$ into $\hat{\rho}(t_b)$ (with $t_b > t_a$) is written $\hat{\mathbf{U}}(t_b, t_a)$.

The propagator is a unitary operator (*2–6, 29*), from which follows that its inverse may be obtained by the adjoint operation (see Eq. [4]):

$$\hat{\mathbf{U}}(t_b, t_a)^{-1} = \hat{\mathbf{U}}(t_b, t_a)^{\dagger} \qquad [119]$$

The propagator is formally related to the Hamiltonian through the *Schrödinger equation* (*2–6, 29*)

$$\frac{d}{dt}\hat{\mathbf{U}}(t, t_a) = -i\hat{\mathbf{H}}(t)\hat{\mathbf{U}}(t, t_a) \qquad [120]$$

This differential equation needs to first be solved for an expression of $\hat{\mathbf{U}}(t_b, t_a)$, which *subsequently* can be used in Eq. [118]. However, the Schrödinger equation generally has no exact solution. This is one reason why computer programs that numerically carry out the integration are useful. On the other hand, in the case of dynamically inhomogeneous Hamiltonians, Eq. [120] may be solved analytically. We will demonstrate this in a later section.

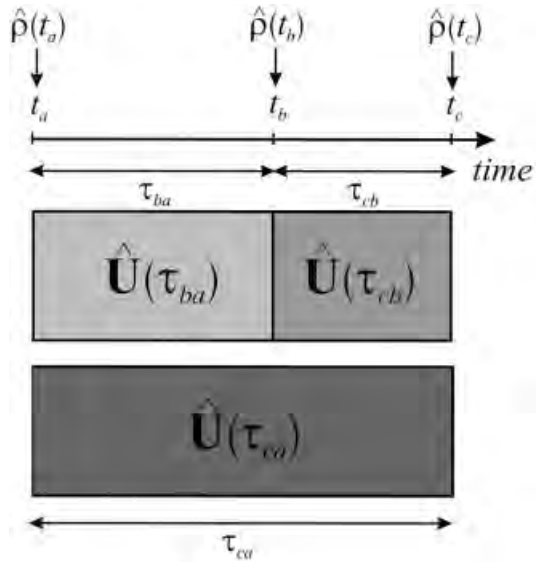

Figure 9 A propagator $\hat{\mathbf{U}}(\tau_{ca})$, which is schematically depicted as the shaded box at the bottom of the figure, is to be determined over the time interval $\tau_{ca} = t_c - t_a$. This propagator may be formed by first dividing the interval τ_{ca} into two smaller segments, $\tau_{ba} = t_b - t_a$ and $\tau_{cb} = t_c - t_b$, and then calculating $\hat{\mathbf{U}}(\tau_{ca})$ as the time-ordered product $\hat{\mathbf{U}}(\tau_{ca}) = (\hat{\mathbf{U}}\tau_{cb})\ \hat{\mathbf{U}}(\tau_{ba})$ from the propagators over the smaller time segments. Note the order of the operators in the product. If the expression for $\hat{\rho}(t_a)$ is known, each of these propagators may then be used to determine the density operators $\hat{\rho}(t_b)$ and $\hat{\rho}(t_c)$ according to the operator sandwich formula, Eq. [118].

Properties of Propagators

In this section we discuss a few important properties of propagators, which will prove very useful in numerical implementations.

Assume that the Schrödinger equation is integrated over the interval $\tau_{ca} = t_c - t_a$, with $t_c > t_a$ as illustrated in Fig. 9. By definition, the solution is the propagator $\hat{\mathbf{U}}(t_c, t_a) \equiv \hat{\mathbf{U}}(\tau_{ca})$, which transforms $\hat{\rho}(t_a)$ into $\hat{\rho}(t_c)$ through the operator sandwich, Eq. [118]. At the moment, we do not consider *how* the propagator is determined. Here we introduce the shorthand notation $\hat{\mathbf{U}}(\tau_{ca})$: in the following, we will use the two notations $\hat{\mathbf{U}}(t_c, t_a)$ and $\mathbf{U}(\tau_{ca})$ interchangeably.

If a time point t_b is picked within the interval τ_{ca}, we may solve the Shrödinger equation separately over each of the two time segments τ_{ba} and τ_{cb} of Fig. 9. This results in $\hat{\mathbf{U}}(t_b, t_a) \equiv \hat{\mathbf{U}}(\tau_{ba})$ [transforming $\hat{\rho}(t_a) \rightarrow \hat{\rho}(t_b)$] and $\hat{\mathbf{U}}(t_c, t_b) \equiv \hat{\mathbf{U}}(\tau_{cb})$ [transforming $\hat{\rho}(t_b) \rightarrow \hat{\rho}(t_c)$]. The following relationship holds between the three operators, $\hat{\mathbf{U}}(t_c, t_a)$, $\hat{\mathbf{U}}(t_b, t_a)$, and $\hat{\mathbf{U}}(t_c, t_b)$ (*29*):

$$\hat{\mathbf{U}}(t_c, t_a) = \hat{\mathbf{U}}(\tau_{cb})\hat{\mathbf{U}}(\tau_{ba}) \quad [121]$$

$$= \hat{\mathbf{U}}(t_c, t_b)\hat{\mathbf{U}}(t_b, t_a) \quad [122]$$

The *order* of the propagators in the product $\hat{\mathbf{U}}(t_c, t_b)\hat{\mathbf{U}}(t_b, t_a)$ is important and may not be changed, because the operators generally do not commute. A product of the form of Eq. [122] is said to be *time ordered* (*1–5*): propagators involving *later* time points appear to the *left* to those involving earlier time points.

We motivate Eq. [122] as follows: if we are to propagate the density operator from $t = t_a$ to $t = t_c$, we may *either* do the transformation in *one step* using the operator of the left-hand side of Eq. [122] according to

$$\hat{\rho}(t_c) = \hat{\mathbf{U}}(t_c, t_a)\hat{\rho}(t_a)\hat{\mathbf{U}}(t_c, t_a)^\dagger \quad [123]$$

or through *two successive transformations* using the right-hand side of Eq. [122]. We verify that the sandwich

$$\{\hat{\mathbf{U}}(t_c, t_b)\hat{\mathbf{U}}(t_b, t_a)\}\hat{\rho}(t_a)\{\hat{\mathbf{U}}(t_c, t_b)\hat{\mathbf{U}}(t_b, t_a)\}^\dagger \quad [124]$$

is indeed equal to the density operator $\hat{\rho}(t_c)$. Using the fact that the adjoint of a product of two unitary operators is equal to the *reversed* product involving the adjoint of each operator (*6, 29*), that is,

$$\{\hat{\mathbf{A}}\hat{\mathbf{B}}\}^\dagger = \hat{\mathbf{B}}^\dagger\hat{\mathbf{A}}^\dagger \quad [125]$$

it follows that the rightmost factor of Eq. [124] corresponds to $\{\hat{\mathbf{U}}(t_c, t_b)\hat{\mathbf{U}}(t_b, t_a)\}^\dagger = \hat{\mathbf{U}}(t_b, t_a)^\dagger\hat{\mathbf{U}}(t_c, t_b)^\dagger$. Hence, we may write

$$\hat{\mathbf{U}}(t_c, t_b)\hat{\mathbf{U}}(t_b, t_a) \cdot \hat{\rho}(t_a) \cdot \hat{\mathbf{U}}(t_b, t_a)^\dagger\hat{\mathbf{U}}(t_c, t_b)^\dagger$$
$$= \hat{\mathbf{U}}(t_c, t_b) \cdot \underbrace{\hat{\mathbf{U}}(t_b, t_a)\hat{\rho}(t_a)\hat{\mathbf{U}}(t_b, t_a)^\dagger}_{\hat{\rho}(t_b)} \cdot \hat{\mathbf{U}}(t_c, t_b)^\dagger \quad [126]$$

Inserting Eq. [118] into Eq. [126] gives $\hat{\mathbf{U}}(t_c, t_b)\hat{\rho}(t_b)\hat{\mathbf{U}}(t_c, t_b)^\dagger$, which, by definition, equals $\hat{\rho}(t_c)$. Hence, the right-hand side of Eq. [122] effects the transformation $\hat{\rho}(t_a) \rightarrow \hat{\rho}(t_c)$.

In general, if the density operator is to be propagated over a given time interval τ_{ca}, the result is the same, regardless of whether the propagator $\hat{\mathbf{U}}(t_c, t_a)$ is used directly or a series of "small-step" transformations (involving propagators over smaller time segments within τ_{ca}) are used successively.

Time propagation of the density operator, that is, transforming $\hat{\rho}(t_a) \rightarrow \hat{\rho}(t_c)$ in successive steps, is analogous to a series of geometrical transformations in 3-dimensional space, that is, transforming an object by a sequence of rotation operators $\hat{\mathbf{R}}(\Omega_{FF'})$. In the former case, the propagator $\hat{\mathbf{U}}(t_c, t_a)$ may be decomposed into a product of propagators over subsegments of τ_{ca}, according to Eq. [122]. In the latter case, a *net* rotation operator may be decomposed into a product of rotation operators (each effecting a "simpler rotation") as illustrated by Eq. [39].

Another important property of propagators is that $\hat{\mathbf{U}}(t_a, t_b)$ is the inverse of $\hat{\mathbf{U}}(t_b, t_a)$, that is,

$$\hat{\mathbf{U}}(t_a, t_b) = \{\hat{\mathbf{U}}(t_b, t_a)\}^{-1} = \hat{\mathbf{U}}(t_b, t_a)^\dagger \quad [127]$$

Note the ordering of time points. If $t_b > t_a$, the meaning of $\hat{\mathbf{U}}(t_a, t_b)$ is the operator that transforms the density operator *backward* in time: $\hat{\rho}(t_b) \rightarrow \hat{\rho}(t_a)$. Equation [127] may be proven as follows: assume that we first transform $\hat{\rho}(t_a)$ into $\hat{\rho}(t_b)$ according to Eq. [118]. Next, we perform the *reverse* transformation $\hat{\rho}(t_b) \rightarrow \hat{\rho}(t_a)$ according to

$$\hat{\rho}(t_a) = \hat{\mathbf{U}}(t_a, t_b)\hat{\rho}(t_b)\hat{\mathbf{U}}(t_a, t_b)^\dagger \quad [128]$$

By combining both transformations sequentially, we get the following result:

$$\hat{\rho}(t_a) = \hat{\mathbf{U}}(t_a, t_b) \cdot \underbrace{\hat{\rho}(t_b)}_{\hat{\mathbf{U}}(t_b, t_a)\hat{\rho}(t_a)\hat{\mathbf{U}}(t_b, t_a)^\dagger} \cdot \hat{\mathbf{U}}(t_a, t_b)^\dagger \quad [129]$$

$$= \{\hat{\mathbf{U}}(t_a, t_b)\hat{\mathbf{U}}(t_b, t_a)\}\hat{\rho}(t_a)\{\hat{\mathbf{U}}(t_a, t_b)\hat{\mathbf{U}}(t_b, t_a)\}^\dagger \quad [130]$$

Because the left-hand and right-hand sides of Eq. [130] must be equal, it follows that each of the operator products within braces must be equal to the unity operator,

$$\hat{\mathbf{U}}(t_a, t_b)\hat{\mathbf{U}}(t_b, t_a) = \hat{1} \quad [131]$$

which proves Eq. [127]. The procedure employed to demonstrate Eq. [127] also has an analogy to rotations in space: an object stays unaffected if it is first rotated by an angle θ around a given axis and subsequently rotated by the angle $-\theta$ around the same axis.

NMR Signal

The previous sections explained how the ensemble of spin systems are represented by a density operator and how the Hamiltonian causes the density operator to evolve in time through the propagator. We now continue to discuss the relationship between the density operator and the NMR time-domain signal.

The acquired NMR time-domain signal $s(t)$ corresponds to the *expectation value* $\langle\hat{\mathbf{Q}}\rangle$ of an "observable operator" $\hat{\mathbf{Q}}$. In principle, $\hat{\mathbf{Q}}$ may be any Hermitian spin operator, because we may only directly detect quantized systems through Hermitian operators (*29*). The time-domain signal $s(t) = \langle\hat{\mathbf{Q}}\rangle(t)$ may be calculated from the trace of the product between the density operator and the observable operator:

$$s(t) = \langle\hat{\mathbf{Q}}\rangle(t) = \mathrm{Tr}\{\hat{\rho}(t)\hat{\mathbf{Q}}\} \qquad [132]$$

The trace of an operator corresponds to the sum of its diagonal elements (*29*). Using an arbitrary basis set, the time-domain signal may be alternatively expressed in either of the following forms:

$$s(t) = \sum_{j=1}^{\mathcal{N}} \langle j|\hat{\rho}\hat{\mathbf{Q}}|j\rangle \qquad [133]$$

$$s(t) = \sum_{j,k=1}^{\mathcal{N}} \langle j|\hat{\rho}|k\rangle\langle k|\hat{\mathbf{Q}}|j\rangle \qquad [134]$$

Using Eq. [133], the signal is calculated by taking the trace of the product $\hat{\rho}\hat{\mathbf{Q}}$, while Eq. [134] implements the trace as a pairwise multiplication of elements of the two operators. The latter expression follows after inserting the closure relation into Eq. [133]; a similar calculation was performed earlier.

Modern NMR spectrometers employ *quadrature detection*, which results in detection of -1QC (*4–6, 35*). In practice, this is performed by simultaneously recording the expectation values of the two Hermitian operators $\langle\hat{\mathbf{I}}_x\rangle(t)$ and $\langle\hat{\mathbf{I}}_y\rangle(t)$. Next, they are combined using Eqs. [75] and [76] to obtain the expectation value $\langle\hat{\mathbf{I}}^+\rangle(t)$. Therefore, $\hat{\mathbf{I}}^+$ *corresponds to the detection of* $-1QC$, despite the fact that formally, this operator is not Hermitian (as may be seen from its matrix representation). We refer to Refs. (*4–6, 35*) for more complete accounts of quadrature detection.

Single Pulse Experiment. Assume an RF pulse of flip angle $\pi/2$ and phase $\pi/2$ [denoted $(\pi/2)_y$, see Refs. (*2–6*)] is applied to an ensemble of nuclear spins at thermal equilibrium in a strong magnetic field. Before the pulse is initiated, there is a net spin polarization pointing along the static field. The pulse rotates this polarization around the rotating frame y axis by the angle $\pi/2$, leaving the net polarization pointing along the rotating frame x axis right after the pulse. This corresponds to the following density operator

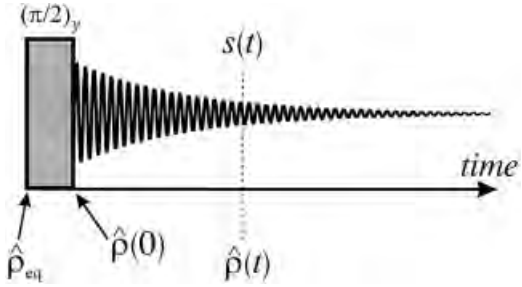

Figure 10 A radio frequency pulse scheme for a simple NMR experiment generating a detectable NMR time-domain signal. The spin ensemble is initially at thermal equilibrium, corresponding to the density operator $\hat{\rho}_{eq} = \hat{\mathbf{I}}_z$. A $\pi/2$ pulse is applied along the y axis of the rotating frame, creating observable single-quantum coherences ("transverse magnetization"). The NMR signal acquisition starts right after the pulse and defines $t = 0$. At this time point, the density operator is given by $\hat{\rho}(0) = \hat{\mathbf{I}}_x = \hat{\mathbf{I}}^+ + \hat{\mathbf{I}}^-$, where the presence of $+1$QC and -1QC is signified by the operators $\hat{\mathbf{I}}^+$ and $\hat{\mathbf{I}}^-$, respectively. The subsequent *evolution of the* $-1Q$ *coherences generates the NMR time-domain signal* (here illustrated by a damped oscillating function), as discussed in the text. The figure is not drawn to scale: the duration of the pulse is on the order of microseconds whereas the signal acquisition interval is normally in the range of tens or hundreds of milliseconds.

$$\hat{\rho}(t_0) = \hat{\mathbf{I}}_x \qquad [135]$$

Because $\hat{\mathbf{I}}_x$ has off-diagonal elements (as may be verified from its matrix representation, Eq. [78]) it represents a spin ensemble state of single-quantum coherences. As discussed above, single-quantum coherences may be interpreted as transverse magnetization, which may be detected by the NMR spectrometer. The NMR time-domain signal generated by the subsequent spin evolution under the Hamiltonian is usually referred to as a free-induction decay (*2–6*). The time point at the start of NMR signal acquisition is denoted t_0, and it is furthermore defined to be equal to zero (*2–6*). Figure 10 depicts the RF scheme of the pulse and the corresponding changes of the density operator. Assuming that the time-domain signal is acquired by this simple one-pulse experiment, its corresponding NMR frequency-domain spectrum $S(\omega)$ is obtained by Fourier transforming $s(t)$ using Eq. [28], as discussed previously.

Equations [118], [120], and [132] are the fundamental expressions for calculating the NMR time-domain signal from *any* experiment. However, these equations are very general and in their present form do not provide much insight into the dynamics. The following sections discuss how they are applied to so-called "dynamically inhomogeneous problems"

and how the properties of the resulting NMR signals in the time and frequency domains are derived. The resulting equations will be implemented numerically in my next article.

It should be kept in mind that the spin Hamiltonian, density matrix, and NMR signal are not only dependent on time but also on the spatial orientation of the molecule: For brevity, this dependence has not been indicated explicitly, but it will be included in a following article. Another factor that needed to be taken into account in a numerical simulation is relaxation of the nuclear spins: we do not include this explicitly, but the damping of the spin coherences (T_2 or spin–spin relaxation) is accounted for phenomenologically, as discussed later.

DYNAMICALLY HOMOGENEOUS AND INHOMOGENEOUS HAMILTONIANS

The crucial step in NMR simulations is the numerical integration of the Shrödinger equation (Eq. [120]). Therefore, perhaps the most important factor dictating both the complexity of computer implementation (i.e., the code) and the time span when executing the simulation is the nature of the Hamiltonian under which the spins evolve.

If the Hamiltonian does not commute with itself when evaluated at two different time points, that is, if

$$[\hat{\mathbf{H}}(t_1), \hat{\mathbf{H}}(t_2)] = \hat{\mathbf{H}}(t_1)\hat{\mathbf{H}}(t_2) - \hat{\mathbf{H}}(t_2)\hat{\mathbf{H}}(t_1) \neq 0 \qquad [136]$$

the Schrödinger equation generally has no simple analytical solution. The following article will outline how $\hat{\mathbf{U}}(t, t_0)$ may be approximated numerically in such cases. This article is primarily confined to dealing with somewhat simpler problems: those for which the Hamiltonian is either *time-independent* or *self-commuting and periodic* in time.

If the Hamiltonian is time independent ($\hat{\mathbf{H}}$ = constant), the propagator, which is obtained as the solution to Eq. [120], is given by the simple expression

$$\hat{\mathbf{U}}(t, t_0) = \exp\{-i(t - t_0)\hat{\mathbf{H}}\} \qquad [137]$$

This allows the obtaining of the density operator, and hence the time signal, at any point in time by the evaluation of an exponential operator, which can be easily done using the results presented earlier. An experiment with a static sample is a typical example of such a case.

Maricq and Waugh (*27*) introduced the nomenclature *dynamically inhomogeneous* Hamiltonian when it is self-commuting and *dynamically homogeneous* when it is not self-commuting. In the former case, $[\hat{\mathbf{H}}(t_1), \hat{\mathbf{H}}(t_2)] = 0$. Physically, the spin evolution under a sum of mutually commuting Hamiltonians (i.e., the dynamically inhomogeneous case) is the superposition of the evolution under each interaction taken in isolation: the various interactions "add up." However, if these Hamiltonians do not commute (i.e., the dynamically homogeneous case), the net evolution is more complicated because of interference between the various terms. An important point is that the total Hamiltonian is dynamically homogeneous, even if all individual Hamiltonians commute with each other except *at least one* (*27*).

Consequently, it is necessary to identify each experimental situation that is to be simulated numerically and determine whether its Hamiltonian is homogeneous or inhomogeneous. This depends both on the "internal" interactions within the spin system and on the experimental conditions (MAS and RF fields). The Hamiltonians for experiments with *rotating solids* are dynamically homogeneous in general. However, there are some important exceptions. Examples of dynamically inhomogeneous cases in rotating solids are isolated nuclear spins subject to chemical shift anisotropy and/or first-order quadrupolar interactions. Heteronuclear spin systems also evolve under dynamically inhomogeneously Hamiltonians, as long as the spins are not subject to second-order quadrupolar interactions or homonuclear couplings: the heteronuclear dipolar or *J*-coupling Hamiltonians commute with the chemical shifts or first-order quadrupolar Hamiltonians, as can be verified using the expressions of the spin operators given in Table 2. Furthermore, as discussed in Ref. (*4*), special cases exist in rotating solids where the spin operators of the interactions do not commute with each other, but which are nevertheless dynamically inhomogeneous because all spatial tensor orientations coincide. One example is a *linear* chain of homonuclear dipolar-coupled spins with identical chemical shift tensors.

Note, however, that all the cases mentioned above are dynamically inhomogeneous *only* in the *absence* of RF fields: the rotating frame RF Hamiltonian during a pulse (applied exactly on resonance) of constant amplitude ω_{RF} and phase ϕ_{RF} may be written (*1–6*)

$$\hat{\mathbf{H}}_{RF} = \omega_{RF}(\hat{\mathbf{I}}_x\cos\{\phi_{RF}\} + \hat{\mathbf{I}}_y\sin\{\phi_{RF}\}) \qquad [138]$$

It may be verified that $\hat{\mathbf{H}}_{\mathrm{RF}}$ does not commute with the internal spin interactions listed in Table 2 and hence will lead to homogeneous spin dynamics.

NMR TIME SIGNAL AND SPECTRUM FROM DYNAMICALLY INHOMOGENEOUS HAMILTONIAN

General Formalism

Here we derive the general expression for the NMR time-domain signal (Eq. [132]) from spin systems evolving under dynamically inhomogeneous Hamiltonians. Similar treatments may be found, for example, in Refs. (*2, 4, 36*). For most equations, we keep the arbitrary initial time point t_0 for completeness (e.g., in Eqs. [118] and [120]), but we always assume that $t_0 = 0$ (corresponding to the start of acquisition in an NMR experiment) when evaluating the NMR signal. We employ a rotating frame in the analysis and assume the absence of RF fields during the acquisition.

Dynamically Inhomogeneous Hamiltonians. Dynamically inhomogeneous Hamiltonians have, in general, time-dependent eigenvalues but time-independent eigenstates (eigenvectors) (*27*). Consequently, if the Hamiltonian is diagonalized, a set of $\mathcal{N}$ eigenvalues ω_u and $\mathcal{N}$ orthonormal eigenstates $|u\rangle$ is obtained, where each state obeys the following eigenequation:

$$\hat{\mathbf{H}}(t)|u\rangle = \omega_u(t)|u\rangle \qquad [139]$$

We reserve the label u (and when needed v, r, and s) for indices representing eigenstates and eigenvalues of the *Hamiltonian* or its corresponding propagator. As for any operator represented in its eigenbasis (Eq. [7]), the Hamiltonian may be expanded as products of an eigenvalue $\omega_u(t)$ and a projection operator $|u\rangle\langle u|$ onto the corresponding eigenstate $|u\rangle$ (*2, 4, 36*)

$$\hat{\mathbf{H}}(t) = \sum_{u=1}^{\mathcal{N}} \omega_u(t)|u\rangle\langle u| \qquad [140]$$

Propagator and Dynamic Phase. Next we seek an expression for the propagator. If the Hamiltonian commutes with itself at all time points between t_0 and t (as in the present case), the formal solution to Eq. [120] is obtained as the exponential of the integral of the Hamiltonian over the time interval $t_0 \leq t' \leq t$,

$$\hat{\mathbf{U}}(t, t_0) = \exp\left\{-i \int_{t_0}^{t} dt' \hat{\mathbf{H}}(t')\right\} \qquad [141]$$

$$= \exp\left\{-i \sum_{u=1}^{\mathcal{N}} \int_{t_0}^{t} \omega_u(t')dt'|u\rangle\langle u|\right\} \qquad [142]$$

where the last equality follows by inserting Eq. [140]. Equation [142] shows that the propagator corresponds to a sum over complex exponentials of integrated Hamiltonian eigenvalues, each multiplied with the projection operator $|u\rangle\langle u|$. We define the real-valued function $\Phi_u(t, t_0)$ as the integrated eigenvalue $\omega_u(t)$ over the time interval

$$\Phi_u(t, t_0) = \int_{t_0}^{t} dt' \omega_u(t') \qquad [143]$$

The symbol $\Phi_u(t, t_0)$ is called the *dynamic phase* (*4, 36–38*) accumulated by the eigenstate $|u\rangle$ over the time interval $t_0 \leq t' \leq t$. The dynamic phases involve products of Hamiltonian eigenvalues (rads^{-1}) and time (s); hence, $\Phi_u(t, t_0)$ is in rad units, which means it may be interpreted as an "angle." We elaborate on this physical interpretation further later when considering the time evolution of the density operator and the form of the time-domain signal. From the properties of the integral it follows that the dynamic phase $\Phi_u(t_0, t)$ is related to $\Phi_u(t, t_0)$ by sign reversal:

$$\Phi_u(t_0, t) \equiv \int_{t}^{t_0} dt' \omega_u(t') = -\int_{t_0}^{t} dt' \omega_u(t')$$

$$\equiv -\Phi_u(t, t_0) \qquad [144]$$

By Taylor expansion of the exponential operator $\exp\{i\hat{\mathbf{A}}\}$ (Eq. [13]) one can show that it commutes with $\hat{\mathbf{A}}$, and consequently the two operators share the same eigenbasis (*29*). It then follows that the propagator is diagonal in the Hamiltonian eigenbasis, and Eq. [142] may be expressed in terms of dynamic phases $\Phi_u(t, t_0)$ and projection operators $|u\rangle\langle u|$ as (*4, 36*)

$$\hat{\mathbf{U}}(t, t_0) = \sum_{u=1}^{\mathcal{N}} \exp\{-i\Phi_u(t, t_0)\}|u\rangle\langle u| \quad [145]$$

which is a relatively simple expression. Equation [145] is proven in Appendix B. The inverse propagator $\hat{\mathbf{U}}(t, t_0)^\dagger$, is given by

$$\hat{\mathbf{U}}(t, t_0)^\dagger = \sum_{u=1}^{\mathcal{N}} \exp\{i\Phi_u(t, t_0)\}|u\rangle\langle u| \quad [146]$$

Hence, the operators $\hat{\mathbf{U}}(t, t_0)^\dagger$ and $\hat{\mathbf{U}}(t, t_0)$ only differ by the sign of their exponents.

Time Evolution of Density Operator. We may get more insight into the role of the dynamic phase in spin dynamics by examining the time evolution of the density operator that the propagator of Eq. [145] generates: assume that the density operator is initially proportional to an arbitrary operator $|u\rangle\langle v|$: $\hat{\rho}(t_0) = |u\rangle\langle v|$. This operator is associated with a coherence between the Hamiltonian eigenstates $|u\rangle$ and $|v\rangle$.

The density operator at a later time point t is obtained by combining Eqs. [145] and [118] as follows:

$$\hat{\rho}(t) = \hat{\mathbf{U}}(t, t_0)\hat{\rho}(t_0)\hat{\mathbf{U}}(t, t_0)^\dagger \quad [147]$$

$$= \sum_{r,s=1}^{\mathcal{N}} \underbrace{\exp\{-i\Phi_r(t, t_0)\}|r\rangle\langle r|}_{\hat{\mathbf{U}}(t, t_0)}$$

$$\times \underbrace{|u\rangle\langle v|}_{\hat{\rho}(t_0)} \cdot \underbrace{\exp\{i\Phi_s(t, t_0)\}|s\rangle\langle s|}_{\hat{\mathbf{U}}(t, t_0)^\dagger} \quad [148]$$

$$= \sum_{r,s=1}^{\mathcal{N}} \exp\{-i\Phi_r(t, t_0)\}\exp\{i\Phi_s(t, t_0)\}|r\rangle$$

$$\times \langle r|u\rangle \cdot \langle v|s\rangle \cdot \langle s| \quad [149]$$

Because the Hamiltonian eigenstates are orthonormal, we may use Eq. [2]: $\langle r|u\rangle = \delta_{ru}$ and $\langle v|s\rangle = \delta_{vs}$. The sum then reduces to the single term

$$\hat{\rho}(t) = \exp\{-i\Phi_u(t, t_0)\}\exp\{i\Phi_v(t, t_0)\} \cdot |u\rangle\langle v| \quad [150]$$

$$= \exp\{i\Phi_{uv}(t, t_0)\}|u\rangle\langle v| \quad [151]$$

where the two exponents were combined into the phase $\Phi_{uv}(t, t_0)$, defined as the difference between the dynamic phases of states $|v\rangle$ and $|u\rangle$,

$$\Phi_{uv}(t, t_0) = \Phi_v(t, t_0) - \Phi_u(t, t_0) \quad [152]$$

Note how the difference is formed: the phase corresponding to the leftmost index (u) is subtracted from that to the right (v). In the following, we employ similar indexing to denote differences between other entities.

Equation [151] shows that the density operator remains proportional to the operator $|u\rangle\langle v|$ at all time points. All changes are accommodated in the phase factor $\exp\{i\Phi_{uv}(t, t_0)\}$. The spin dynamics under a dynamically inhomogeneous Hamiltonian is remarkably simple; if the spin ensemble is initially in a certain state, it stays there at all times. We stress that Eq. [151] is a direct consequence of having *time-independent* Hamiltonian eigenstates. All manipulations leading to Eq. [151] implicitly exploited that the eigenstates of the Hamiltonian and propagator are independent of time.

A homogeneous Hamiltonian, on the other hand, has *time-dependent* eigenstates: the corresponding propagator (i.e., the solution of Eq. [120]) generally has no closed analytical form. Assume that the density operator is initially proportional to $|u\rangle\langle v|$ (representing a certain coherence in the spin ensemble) and subject to a dynamically homogeneous Hamiltonian. At a later time point, this coherence will generally be transferred into other coherences and populations, depending on the exact form of the Hamiltonian. The density operator at a given time point may always be expressed as a linear combination of its eigenstates. However, these are time *dependent* for dynamically homogeneous Hamiltonians.

NMR Time-Domain Signal. In this section we derive the general expression for the NMR time-domain signal from a dynamically inhomogeneous Hamiltonian (Eq. [159]) for $t_0 = 0$.

The time-domain signal is calculated as the trace of the product of the density and observable operators (Eq. [133]). The trace of an operator (or products of operators) is independent of the choice of basis set for the matrix representation (*3, 4, 29*): we employ the eigenbasis of the Hamiltonian, leading to

$$s(t) = \sum_{u=1}^{\mathcal{N}} \langle u|\hat{\rho}(t)\hat{\mathbf{Q}}|u\rangle \quad [153]$$

Next we use the idea that the basis set is orthonormal and insert the closure identity (Eq. [112]):

$$s(t) = \sum_{u,v=1}^{\mathcal{N}} \langle u|\hat{\rho}(t)\underbrace{|v\rangle\langle v|}_{\hat{1}}\hat{\mathbf{Q}}|u\rangle \qquad [154]$$

which may be compared with a similar expression, Eq. [134], that employed an arbitrary basis set. After inserting Eq. [118], together with the analytical expression for the dynamically inhomogeneous propagator (Eq. [145]), the signal may be expressed as

$$s(t) = \sum_{u,v=1}^{\mathcal{N}} \langle u|\hat{\mathbf{U}}(t,0)\hat{\rho}(0)\hat{\mathbf{U}}(t,0)^{\dagger}|v\rangle\langle v|\hat{\mathbf{Q}}|u\rangle \qquad [155]$$

$$= \sum_{u,v,r,s=1}^{\mathcal{N}} \langle u|\cdot\underbrace{\exp\{-i\Phi_r(t,0)\}|r\rangle\langle r|}_{\hat{\mathbf{U}}(t,0)} \qquad [156]$$

$$\times\,\hat{\rho}(0)\cdot\underbrace{\exp\{i\Phi_s(t,0)\}|s\rangle\langle s|}_{\hat{\mathbf{U}}(t,0)^{\dagger}}\cdot|v\rangle\langle v|\hat{\mathbf{Q}}|u\rangle$$

Rearranging the exponential factors and using Eq. [152] gives

$$s(t) = \sum_{u,v,r,s=1}^{\mathcal{N}} \langle r|\hat{\rho}(0)|s\rangle\cdot\langle v|\hat{\mathbf{Q}}|u\rangle \qquad [157]$$

$$\times\,\exp\{i\Phi_{rs}(t,0)\}\cdot\langle u|r\rangle\cdot\langle s|v\rangle$$

Equating the scalar products $\langle u|r\rangle$ and $\langle s|v\rangle$ with the Kronecker delta functions $\delta(u, r)$ and $\delta(s, v)$, respectively, provides the following expression for the time signal

$$s(t) = \sum_{u,v,r,s=1}^{\mathcal{N}} \langle r|\hat{\rho}(0)|s\rangle$$

$$\times\,\langle v|\hat{\mathbf{Q}}|u\rangle\exp\{i\Phi_{rs}(t,0)\}\delta(u,r)\delta(s,v) \qquad [158]$$

$$= \sum_{u,v=1}^{\mathcal{N}} \langle u|\hat{\rho}(0)|v\rangle\langle v|\hat{\mathbf{Q}}|u\rangle\exp\{i\Phi_{uv}(t,0)\} \qquad [159]$$

Equation [159] is the key result of this section: it corresponds to the *general expression for the NMR time-domain signal from a spin system evolving under a dynamically inhomogeneous Hamiltonian*. Below we examine how it is evaluated in two limiting cases: when the Hamiltonian is either *time-independent* or *periodic* in time. These correspond to the situation of static and rotating samples, respectively, and they are the scenarios considered in the numerical simulations in subsequent articles.

Time-Independent Hamiltonian

Because the Hamiltonian has time-independent eigenvalues, the expression for the dynamic phase $\Phi_{uv}(t, 0)$ evaluates to the simple expression

$$\Phi_{uv}(t,0) = \int_0^t dt'(\omega_v - \omega_u) \qquad [160]$$

$$= \underbrace{(\omega_v - \omega_u)}_{\omega_{uv}}\cdot t \qquad [161]$$

where we defined the frequency ω_{uv} as the eigenvalue difference,

$$\omega_{uv} = \omega_v - \omega_u \qquad [162]$$

By defining an amplitude as the product of the matrix elements of the initial density operator and observable,

$$a_{uv} = \langle u|\hat{\rho}(0)|v\rangle\langle v|\hat{\mathbf{Q}}|u\rangle \qquad [163]$$

Equation [159] casts as (*2*, *4*)

$$s(t) = \sum_{u,v=1}^{\mathcal{N}} a_{uv}\exp\{i\omega_{uv}t\} \qquad [164]$$

Thus, the time-domain signal from a time-independent Hamiltonian is given by a sum of complex exponentials oscillating at the angular frequency differences ω_{uv} of the Hamiltonian eigenvalues.

The time-domain signal is converted into the NMR spectrum by a Fourier transform

$$S(\omega) = \sum_{u,v=1}^{\mathcal{N}} a_{uv}\delta(\omega, \omega_{uv}) \qquad [165]$$

Equation [165] shows that the spectrum from a time-independent Hamiltonian is represented by a set of "spikes" (δ functions) at the frequency coordinates $\omega = \omega_{uv}$. The corresponding amplitudes a_{uv} are given as products of the elements of the observable and initial density operator, both expressed in the *eigenbasis* of the Hamiltonian. An experimental spectrum always has "broad" peaks due to decay mechanisms of the time signal ("relaxation"). Assuming an exponential decay of the time-domain signal, the corresponding spectrum that results after Fourier trans-

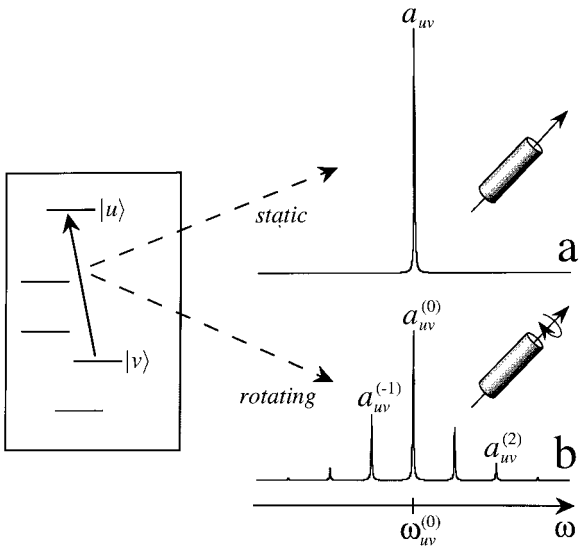

Figure 11 A typical spectrum from (a) time-independent and (b) time-periodic Hamiltonians, corresponding to the case of one single molecular orientation ("single crystal") in static and rotating samples, respectively. Only one transition of the spin system is shown, involving the Hamiltonian eigenstates $\{|u\rangle, |v\rangle\}$. In the static case, the pair of eigenstates generates a *single* spectral peak at the frequency ω_{uv} (given by the difference between the eigenvalues of the states: $\omega_{uv} = \omega_v - \omega_u$) and with the amplitude a_{uv} (Eq. [163]). In the rotating case, the spectrum corresponds to a *side-band manifold*, centered at $\omega_{uv}^{(0)} = \omega_v^{(0)} - \omega_u^{(0)}$, and with the expressions for the frequencies $\omega_{uv}^{(k)}$ and amplitudes $a_{uv}^{(k)}$ of the side bands given by Eqs. [212] and [211], respectively. Two neighboring side bands are separated by the rotational frequency ω_r. In this case, we assumed that $\omega_{uv} = \omega_{uv}^{(0)}$, but this does not generally hold, as explained in the text.

formation contains peaks with Lorentzian shapes instead of δ functions. Line broadening may also be introduced in simulated spectra, as will be explained in the next article. Figure 11(a) shows a typical spectrum obtained from one of the terms in Eq. [165].

Example: Isotropic Chemical Shift Evolution. To illustrate spin evolution under a time-independent Hamiltonian, we explicitly derive the form of the NMR time-domain signal generated from the isotropic chemical shift interaction using the general formalism presented earlier. We will show that the result obtained here is consistent with the expressions for the time signal derived above (Eq. [164]).

Assume an ensemble of isolated spins-$\frac{1}{2}$ prepared in a state of transverse magnetization, generated by a $(\pi/2)_y$ pulse at the start of signal acquisition ($t_0 = 0$), as discussed earlier. This corresponds to an initial density operator proportional to $\hat{\mathbf{I}}_x$, which in turn may be expressed in terms of $\hat{\mathbf{I}}^+$ and $\hat{\mathbf{I}}^-$ using Eq. [75],

$$\hat{\rho}(0) = \hat{\mathbf{I}}_x \qquad [166]$$

$$= \frac{1}{2}(\hat{\mathbf{I}}^+ + \hat{\mathbf{I}}^-) \qquad [167]$$

or, formulated in the Dirac formalism,

$$\hat{\rho}(0) = \frac{1}{2}(|\alpha\rangle\langle\beta| + |\beta\rangle\langle\alpha|) \qquad [168]$$

We assume for simplicity that the spins are only affected by the isotropic chemical shift interaction, corresponding to the Hamiltonian

$$\hat{\mathbf{H}}_{\mathrm{CS,iso}} = \omega_{\mathrm{iso}}\hat{\mathbf{I}}_z \qquad [169]$$

$$= \frac{1}{2}\omega_{\mathrm{iso}}\begin{pmatrix}1 & 0\\ 0 & -1\end{pmatrix} \qquad [170]$$

where we inserted the explicit matrix representation of $\hat{\mathbf{I}}_z$ (Eq. [77]). Because the Hamiltonian is diagonal in the Zeeman basis, its eigenvalues are directly extracted as $\omega_\alpha = \omega_{\mathrm{iso}}/2$ and $\omega_\beta = -\omega_{\mathrm{iso}}/2$. Hence, the eigenequations are

$$\hat{\mathbf{H}}_{\mathrm{CS,iso}}|\alpha\rangle = \frac{1}{2}\omega_{\mathrm{iso}}|\alpha\rangle \qquad [171]$$

$$\hat{\mathbf{H}}_{\mathrm{CS,iso}}|\beta\rangle = -\frac{1}{2}\omega_{\mathrm{iso}}|\beta\rangle \qquad [172]$$

The eigenvalues are time independent, and the expressions for the corresponding dynamic phases $\Phi_\alpha(t, 0)$ and $\Phi_\beta(t, 0)$ are easily calculated from Eq. [143]:

$$\Phi_\alpha(t, 0) = -\Phi_\beta(t, 0) = \frac{1}{2}\omega_{\mathrm{iso}}\int_0^t dt' \qquad [173]$$

$$= \frac{1}{2}\omega_{\mathrm{iso}}t \qquad [174]$$

Applying Eq. [152] to form the dynamic phase differences $\Phi_{\alpha\beta}(t, 0)$ and $\Phi_{\beta\alpha}(t, 0)$ gives

$$\Phi_{\alpha\beta}(t, 0) = \Phi_\beta(t, 0) - \Phi_\alpha(t, 0) \qquad [175]$$

$$= -\omega_{\mathrm{iso}}t \qquad [176]$$

and

$$\Phi_{\beta\alpha}(t, 0) = -\Phi_{\alpha\beta}(t, 0) = \omega_{iso}t \qquad [177]$$

respectively.

Following reasoning identical to the previous section, we obtain an equivalent expression to Eq. [151]:

$$\hat{\rho}(t) = \frac{1}{2}\left(\exp\{i\Phi_{\alpha\beta}(t, 0)\}|\alpha\rangle\langle\beta| + \exp\{i\Phi_{\beta\alpha}(t, 0)\}|\beta\rangle\langle\alpha|\right) \qquad [178]$$

$$= \frac{1}{2}\left(\exp\{-i\omega_{iso}t\}|\alpha\rangle\langle\beta| + \exp\{i\omega_{iso}t\}|\beta\rangle\langle\alpha|\right) \qquad [179]$$

According to Eq. [179], the density operator at the time point t is given by two terms, each being a product of an operator and a time-dependent exponential function involving a dynamic phase. The physical meaning of these terms is that the $+1$Q coherence (represented by $|\alpha\rangle\langle\beta|$) oscillates at the negative value of the isotropic chemical shift $-\omega_{iso}$, whereas the -1Q coherence (represented by $|\beta\rangle\langle\alpha|$) oscillates at $+\omega_{iso}$.

The time-domain signal originating from the time evolution of this spin ensemble is obtained by inserting the expression for the density operator together with the observable $\hat{\mathbf{I}}^{+} = |\alpha\rangle\langle\beta|$ into Eq. [133]:

$$s(t) = \frac{1}{2}\sum_{j=\alpha,\beta}\langle j|\hat{\rho}\hat{\mathbf{Q}}|j\rangle \qquad [180]$$

$$= \frac{1}{2}\sum_{j=\alpha,\beta}\langle j|\cdot\left(\exp\{-i\omega_{iso}t\}|\alpha\rangle\langle\beta|\cdot|\alpha\rangle\underbrace{|\alpha\rangle\langle\beta|}_{\hat{\mathbf{Q}}} + \exp\{i\omega_{iso}t\}|\beta\rangle\langle\alpha|\cdot\underbrace{|\alpha\rangle\langle\beta|}_{\hat{\mathbf{Q}}}\right)\cdot|j\rangle \qquad [181]$$

Again, the orthonormality condition of the basis states proves useful: the first and second product within the parentheses may be simplified as

$$|\alpha\rangle\langle\beta|\cdot|\alpha\rangle\langle\beta| = 0 \qquad [182]$$

and

$$|\beta\rangle\langle\alpha|\cdot|\alpha\rangle\langle\beta| = |\beta\rangle\langle\beta| \qquad [183]$$

respectively. Moreover, the sum over j collapses into a single term

$$s(t) = \frac{1}{2}\exp\{i\omega_{iso}t\} \times \left(\underbrace{\langle\alpha|\cdot|\beta\rangle\langle\beta|\cdot|\alpha\rangle}_{=0} + \underbrace{\langle\beta|\cdot|\beta\rangle\langle\beta|\cdot|\beta\rangle}_{=1}\right) \qquad [184]$$

$$= \frac{1}{2}\exp\{i\omega_{iso}t\} \qquad [185]$$

Note that all contributions from the $+1$QC operator $|\alpha\rangle\langle\beta|$ vanished; this is the mathematical consequence of the fact that quadrature detection implies detection of -1QC. Thus, in the present case, the signal only contains *one* frequency: the isotropic chemical shift ω_{iso}. Subsequent Fourier transformation produces an NMR spectrum corresponding to a single peak at the isotropic chemical shift frequency, as indicated in Fig. 11(a). Note that Eq. [185] conforms to Eq. [164] with the following expressions for the frequency and amplitude: $\omega_{uv} = \omega_{iso}$ and $a_{uv} = 1/2$.

This example represented probably the simplest possible case. However, the calculations outlined in the next section extend the present case by allowing the incorporation of anisotropic chemical shift contributions and heteronuclear dipolar interactions in multispin systems. In all these cases, the spin Hamiltonian is dynamically inhomogeneous and, furthermore, diagonal in the Zeeman product basis. See Ref. (*36*) for a similar calculation that additionally includes the anisotropic chemical shift interaction.

Time-Periodic Self-Commuting Hamiltonian

Here we carry out analogous calculations for a rotating sample as was done for the static case in the previous section. The key steps of the procedure are the same: (i) obtain the Hamiltonian and its eigenvalues; (ii) calculate the expression for the time-dependent dynamic phase $\Phi_{uv}(t, 0)$ originating from each pair of eigenvalues; (iii) insert these results into the expression for the time-domain signal, Eq. [159].

Hamiltonian. The time-dependent dynamically inhomogeneous Hamiltonian is given by a sum over all NMR interactions:

$$\hat{\mathbf{H}}(t) = \sum_{\Lambda}\hat{\mathbf{H}}_{\Lambda}(t) = \sum_{\Lambda}\omega_{\Lambda}(t)\hat{\mathbf{T}}_{\Lambda} \qquad [186]$$

where $\hat{\mathbf{T}}_\Lambda$ represents the spin part of the interaction and the various spin operators mutually commute: $[\hat{\mathbf{T}}_{\Lambda_j}, \hat{\mathbf{T}}_{\Lambda_k}] = 0$. If two operators commute, they share the same eigenbasis and may both be brought into diagonal form in that basis (although the eigenvalues of the operators are generally different) (*29*). From this it follows that all operators in the sum of Eq. [186] are diagonal in the Hamiltonian eigenbasis. Inserting the closure relation (Eq. [112]) both to the left and to the right of Eq. [186] gives

$$\hat{\mathbf{H}}(t) = \sum_{v=1}^{\mathcal{N}} \sum_{\Lambda} \omega_\Lambda(t) \underbrace{|v\rangle\langle v|}_{\hat{1}} \cdot \hat{\mathbf{T}}_\Lambda \cdot \underbrace{|v\rangle\langle v|}_{\hat{1}} \qquad [187]$$

$$= \sum_{v=1}^{\mathcal{N}} \sum_{\Lambda} \omega_\Lambda(t) \langle v|\hat{\mathbf{T}}_\Lambda|v\rangle \cdot |v\rangle\langle v| \qquad [188]$$

Note that $\langle v|\hat{\mathbf{T}}_\Lambda|v\rangle$ represents the matrix element $(\hat{\mathbf{T}}_\Lambda)_{vv}$.

Hamiltonian Eigenvalues. Next we derive the explicit expressions for the Hamiltonian eigenvalues. We may project out the uth Hamiltonian eigenvalue by multiplying Eq. [188] to the left with the "bra" $\langle u|$ and to the right with the "ket" $|u\rangle$, according to

$$\omega_u(t) = \langle u|\hat{\mathbf{H}}(t)|u\rangle = \langle u| \cdot \left\{ \sum_{v=1}^{\mathcal{N}} \sum_{\Lambda} \omega_\Lambda(t) \langle v|\hat{\mathbf{T}}_\Lambda|v\rangle \cdot |v\rangle\langle v| \right\} \cdot |u\rangle \qquad [189]$$

After rearranging the terms and using the orthonormality conditions of the Hamiltonian eigenstates, all terms for which $v \neq u$ vanish, and we obtain

$$\omega_u(t) = \sum_{\Lambda} \omega_\Lambda(t) \langle u|\hat{\mathbf{T}}_\Lambda|u\rangle \qquad [190]$$

As discussed earlier, the anisotropy frequency $\omega_\Lambda(t)$ of the spatial parts of the Hamiltonian are time periodic in a sample rotating at the constant frequency ω_r, Eq. [190] then implies that the Hamiltonian eigenvalues are also periodic with the same period τ_r:

$$\omega_u(t + \tau_r) = \omega_u(t) \qquad [191]$$

They may accordingly be expanded in a Fourier series:

$$\omega_u(t) = \sum_{m=-2}^{2} \omega_u^{(m)} \exp\{im\omega_r t\} \qquad [192]$$

An explicit form of the Fourier components $\omega_u^{(m)}$ may be obtained by inserting Eq. [104] into Eq. [190] as follows:

$$\omega_u(t) = \sum_{\Lambda} \sum_{m=-2}^{2} \underbrace{\omega_\Lambda^{(m)} \langle u|\hat{\mathbf{T}}_\Lambda|u\rangle}_{\omega_u^{(m)}} \exp\{im\omega_r t\} \qquad [193]$$

and equating the Fourier coefficients with those of Eq. [192]. This is possible since a Fourier series is *unique*, meaning that the Fourier *coefficients* of the two expansions must be *equal*, providing the following relationship between the Fourier components of the eigenvalues and those of the spatial tensors:

$$\omega_u^{(m)} = \sum_{\Lambda} \omega_\Lambda^{(m)} \langle u|\hat{\mathbf{T}}_\Lambda|u\rangle \qquad [194]$$

Thus, the eigenvalue Fourier component $\omega_u^{(m)}$ is given by the sum over the products of the mth Fourier component from each spatial tensor and the matrix element of the corresponding spin tensor operator, expressed in the eigenbasis of the Hamiltonian.

Dynamic Phase. Next we deal with finding an expression for the dynamic phase $\Phi_{uv}(t, t_0)$. To this end, we separate the Hamiltonian eigenvalue in Eq. [192] into time-independent and time-dependent parts as follows:

$$\omega_u(t) = \omega_u^{(0)} + \sum_{m \neq 0} \omega_u^{(m)} \exp\{im\omega_r t\} \qquad [195]$$

Under MAS conditions, $\omega_u^{(0)}$ only contains contributions from the isotropic parts of the spin interactions (represented by zeroth rank tensors) whereas the components $\omega_u^{(m\neq 0)}$ contain only anisotropic parts (represented by components of second rank tensors). The reason that $\omega_u^{(0)}$ is purely isotropic is that all potential contributions from second rank tensors are zero: this follows from Eq. [194] and the fact that $d_{00}^2(\theta_m) = 0$ in the expression for $\omega_\Lambda^{(0)}$ (Eq. [105]). However, for experiments conducted under off-MAS conditions, the Euler angle $\beta_{RL} \neq \theta_m$ and anisotropic contributions will appear in the frequency $\omega_u^{(0)}$. In the following, we ignore such cases.

As discussed below, the separation between isotropic and anisotropic contributions to the eigenvalues

and, subsequently, the dynamic phase, will have implications for the nature of the NMR time-domain signals and frequency-domain spectra obtained from rotating solids.

By combining Eqs. [143] and [195], we obtain the following expression for the dynamic phase $\Phi_u(t, t_0)$:

$$\Phi_u(t, t_0) = \int_{t_0}^{t} dt' \omega_u(t') \qquad [196]$$

$$= \underbrace{\int_{t_0}^{t} dt' \omega_u^{(0)}}_{\omega_u^{(0)}(t-t_0)} + \underbrace{\sum_{m\neq 0} \omega_u^{(m)} \int_{t_0}^{t} dt' \exp\{im\omega_r t'\}}_{\Phi'_u(t,\, t_0)} \qquad [197]$$

As a consequence of the separation of the Hamiltonian eigenvalues into time-independent and time-dependent parts, the dynamic phase $\Phi_u(t, t_0)$ involves the *constant* frequency $\omega_u^{(0)}$ and a *time-dependent* part $\Phi'_u(t, t_0)$:

$$\Phi_u(t, t_0) = \omega_u^{(0)}(t - t_0) + \Phi'_u(t, t_0) \qquad [198]$$

The integration of the exponential functions in $\Phi'_u(t, t_0)$ are easily carried out,

$$\int_{t_0}^{t} dt' \exp\{im\omega_r t'\}$$

$$= (im\omega_r)^{-1}\{\exp\{im\omega_r t\} - \exp\{im\omega_r t_0\}\} \qquad [199]$$

and the following expression for the phase $\Phi'_u(t, t_0)$ is obtained:

$$\Phi'_u(t, t_0) = (i\omega_r)^{-1} \sum_{m\neq 0} m^{-1}\omega_u^{(m)} \times (\exp\{im\omega_r t\} - \exp\{im\omega_r t_0\}) \qquad [200]$$

Note that $\Phi'_u(t, t_0)$ only contains contributions from the *anisotropic* parts of the spin interactions, because Eq. [200] solely comprises components $\omega_u^{(m)}$ with $m \neq 0$: these may only originate from the anisotropic interaction parts expressed by second rank tensors. An interpretation of the Fourier components and the corresponding dynamic phases for a *single interaction* Λ is given in Fig. 12; the dynamic phase $\Phi_u(t, t_0)$ of the Hamiltonian eigenstate $|u\rangle$ is a linear combination of the dynamic phases of the individual interactions $\Phi_\Lambda(t, t_0)$, with the corresponding Fourier components $\omega_u^{(m)}$ and $\omega_\Lambda^{(m)}$ related through Eq. [194].

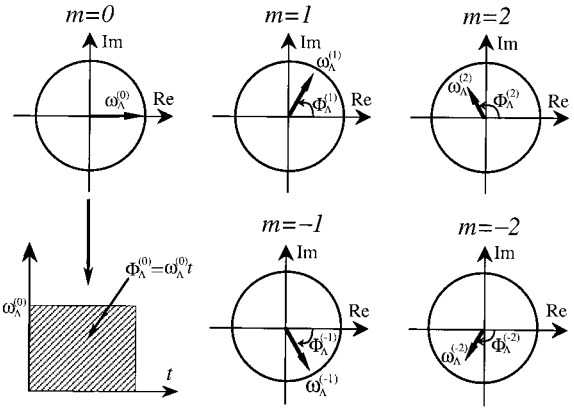

Figure 12 Diagrams illustrating each of the five Fourier components $\omega_\Lambda^{(m)}$ (Eq. [105]) of a spatial tensor in a rotating solid at a given time point t. Each circle corresponds to the plane of complex numbers, and the vectors represent the Fourier components. The component $\omega_\Lambda^{(m)}$ rotates at the velocity $m\omega_r$. Note that the magnitudes (i.e., the lengths of the vectors) are equal for two components with opposite signs of m, but they rotate in opposite directions. At $t = 0$, all vectors are aligned along the real axis; and at every integer multiple of the rotational period, they return to the initial position. The angle $\Phi_\Lambda^{(m)}$ represents the contribution to the dynamic phase accumulated by the component $\omega_\Lambda^{(m)}$. The dynamic phase of a Hamiltonian eigenstate $\Phi_u^{(m)}$ (Eq. [198]) is the sum of contributions from all interactions. The $m = 0$ component $\omega_\Lambda^{(0)}$ is independent of time and stays aligned along the real axis at all times. Its dynamic phase may be visualized as the area beneath the line $y = \omega_\Lambda^{(0)}$ over the interval $0 \leq t' \leq t$.

Next we demonstrate that $\Phi'_u(t, t_0)$ is *periodic*:

$$\Phi'_u(t + \tau_r, t_0) = \Phi'_u(t, t_0) \qquad [201]$$

This may be verified from Eq. [200] by similar arguments that were used to demonstrate that the interaction frequency $\omega_\Lambda^{(t)}$ is periodic. From Eq. [200] we get

$$\Phi'_u(t + \tau_r, t_0) = (i\omega_r)^{-1} \sum_{m\neq 0} m^{-1}\omega_u^{(m)} \times (\exp\{im\omega_r(t + \tau_r)\} - \exp\{im\omega_r t_0\}) \qquad [202]$$

Because the product of the rotational period and the spinning frequency is given by $\omega_r\tau_r = 2\pi$, we find $\exp\{im\omega_r(t + \tau_r)\} = \exp\{im\omega_r t\}\exp\{2im\pi\} =$

$\exp\{im\omega_r t\}$; Eq. [202] reduces to Eq. [200], implying that $\Phi'_u(t + \tau_r, t_0) = \Phi'_u(t, t_0)$.

Finally, we seek an explicit expression for the dynamic phase *difference* $\Phi_{uv}(t, t_0)$. Inserting Eq. [198] (which separates the isotropic and anisotropic contributions of $\Phi_{uv}(t, t_0)$ into Eq. [152] gives

$$\Phi_{uv}(t, t_0) = \{\omega_v^{(0)}(t - t_0) + \Phi'_v(t, t_0)\} - \{\omega_u^{(0)}(t - t_0) + \Phi'_u(t, t_0)\} \quad [203]$$

$$= \omega_{uv}^{(0)}(t - t_0) + \Phi'_{uv}(t, t_0) \quad [204]$$

Analogous to the frequency ω_{uv} in Eq. [162], which is relevant for the static solid, we define the frequency $\omega_{uv}^{(0)}$ as the *difference* between the $m = 0$ *Fourier components* of the Hamiltonian *eigenvalues*:

$$\omega_{uv}^{(0)} = \omega_v^{(0)} - \omega_u^{(0)} \quad [205]$$

Moreover, an explicit expression for the phase difference $\Phi'_{uv}(t, t_0) = \Phi'_v(t, t_0) - \Phi'_u(t, t_0)$ is obtained by using Eq. [200]:

$$\Phi'_{uv}(t, t_0) = (i\omega_r)^{-1} \sum_{m \neq 0} m^{-1}\{\omega_v^{(m)} - \omega_u^{(m)}\} \times (\exp\{im\omega_r t\} - \exp\{im\omega_r t_0\}) \quad [206]$$

NMR Responses in Time and Frequency Domains. Equipped with the expressions derived in the previous subsections, we are prepared for the final step: evaluating the time signal, Eq. [159], in the case of a rotating solid with a self-commuting Hamiltonian. As before, the start of the NMR signal acquisition defines the time origin, $t_0 = 0$.

Exponentiating Eq. [204] provides the following expression for $\exp\{i\Phi_{uv}(t, 0)\}$:

$$\exp\{i\Phi_{uv}(t, 0)\} = \exp\{i\omega_{uv}^{(0)}t\}\exp\{i\Phi'_{uv}(t, 0)\} \quad [207]$$

It corresponds to a product of the exponentiated eigenvalue difference $\omega_{uv}^{(0)}$ and the exponential of the periodic anisotropic phase $\Phi'_{uv}(t, t_0)$. The former is analogous to the factor $\exp\{i\omega_{uv}t\}$ from the static case; both functions comprise a *single frequency*. Note, however, that the frequencies ω_{uv} and $\omega_{uv}^{(0)}$ are in general *not* equal. The frequency ω_{uv} contains both isotropic and anisotropic contributions from the spin interactions, but in the MAS case we arranged that $\omega_{uv}^{(0)}$ only comprises isotropic interactions.

The factor $\exp\{i\Phi'_{uv}(t, 0)\}$ has no counterpart in the case of a static sample; in general, this function comprises an *infinite* number of frequencies, all being harmonics of the rotational frequency ω_r. This may be realized by Fourier expanding the function $\exp\{i\Phi'_{uv}(t, 0)\}$: as expressed by Eq. [27], the complex exponentials of periodic functions (such as the dynamic phase) may be written as a Fourier series, comprising an infinite number of coefficients:

$$\exp\{i\Phi'_{uv}(t, 0)\} = \sum_{k=-\infty}^{\infty} c_{uv}^{(k)}\exp\{ik\omega_r t\} \quad [208]$$

The Fourier coefficient $c_{uv}^{(k)}$ is a function of the Hamiltonian eigenvalue difference $\omega_v^{(m)} - \omega_u^{(m)}$ and hence also depends on the various spatial tensor components; this is realized from the relationships between the dynamic phase, the Hamiltonian eigenvalues, and the interaction parameters, as follows by combining Eqs. [105], [194], and [206]. The coefficients $c_{uv}^{(k)}$ fulfill a normalization condition $\Sigma_k |c_{uv}^{(k)}| = 1$ and may be calculated by Fourier transformation of the function $\exp\{i\Phi'_{uv}(t, 0)\}$. We will discuss this further in following articles.

Finally, by inserting Eqs. [207] and [208] into the general expression for the signal, Eq. [159], we obtain

$$s(t) = \sum_{u,v=1}^{\mathcal{N}} \langle u|\hat{\rho}(0)|v\rangle\langle v|\hat{\mathbf{Q}}|u\rangle\exp\{i\omega_{uv}^{(0)}t\} \times \sum_{k=-\infty}^{\infty} c_{uv}^{(k)}\exp\{ik\omega_r t\} \quad [209]$$

$$= \sum_{u,v=1}^{\mathcal{N}} \sum_{k=-\infty}^{\infty} a_{uv}^{(k)}\exp\{i\omega_{uv}^{(k)}t\} \quad [210]$$

where the amplitudes are given by

$$a_{uv}^{(k)} = \langle u|\hat{\rho}(0)|v\rangle\langle v|\hat{\mathbf{Q}}|u\rangle c_{uv}^{(k)} = a_{uv}c_{uv}^{(k)} \quad [211]$$

and the frequencies by

$$\omega_{uv}^{(k)} = \omega_{uv}^{(0)} + k\omega_r \quad [212]$$

After Fourier transformation of the time signal, the spectrum takes the following form:

$$S(\omega) = \sum_{u,v=1}^{\mathcal{N}} \sum_{k=-\infty}^{\infty} a_{uv}^{(k)}\delta(\omega, \omega_{uv}^{(k)}) \quad [213]$$

Consequently, the spectrum is the sum of contributions from each pair of Hamiltonian eigenstates $|u\rangle$

and $|v\rangle$, each producing a set of spinning *side bands* due to the periodic sample rotation. The side-band manifold is centered at a "fundamental frequency" $\omega_{uv}^{(0)}$ and associated with a frequency separation ω_r between neighboring peaks. This is illustrated in Fig. 11(b).

The origin of the side bands in the rotating case is the periodic exponential function $\exp\{i\Phi'_{uv}(t, 0)\}$. Through Eq. [208] it was shown to correspond to a sum of functions $\exp\{ik\omega_r t\}$, each oscillating at a harmonic $k\omega_r$ of the spinning frequency. Each of these contributes *one* spinning side band to the manifold. However, although the number of side bands is in theory infinite, in practice their amplitudes, $a_{uv}^{(k)} = a_{uv}c_{uv}^{(k)}$, tend to zero for large side-band orders $|k|$. This is because the Fourier components $c_{uv}^{(k)}$ get smaller as the side-band index $|k|$ increases: the *number* of side bands of significant intensity roughly depends on the magnitude of the interaction relative to the spinning frequency, that is, on the ratio $|\omega_\Lambda/\omega_r|$ (*27*). The larger the ratio, the larger the number of side bands in the spectrum. This is seen, for example, from the experimental spectra in Fig. 1(b–d), which were recorded at different spinning frequencies. In the case of several interactions, the ratio involving the sum over all interaction frequencies, $\omega_\Sigma = \Sigma_\Lambda\ \omega_\Lambda$, roughly dictates the number of side bands.

Note that spin evolution under a self-commuting Hamiltonian of the form of Eq. [186] corresponds to an NMR spectrum being a sum of a set of "subspectra," each generated independently from each interaction. For example, consider an isolated ^{13}C—^{1}H segment in an organic molecule under MAS. The ^{13}C spectrum corresponds to a side band manifold, with each side band amplitude arising from the combined effects of the heteronuclear dipolar coupling and the ^{13}C chemical shift anisotropy. In a following article we demonstrate how such a spectrum may be calculated numerically.

The *derivations* in this section assumed dynamically inhomogeneous Hamiltonians under sample spinning conditions, but the *form of the spectrum* given in Eq. [213] holds in the *general* case of spin systems evolving under any time-periodic Hamiltonian, as discussed in Refs. (*18, 20, 39–41*). The appearance of a side-band manifold is a consequence of spin evolution under a *time-periodic* Hamiltonian, regardless of whether this is homogeneous or inhomogeneous. The major difference between these cases is, however, that for dynamically homogeneous Hamiltonians, the total NMR spectrum generated from several interactions is *not* expressible as a superposition of the individual spectra obtained from each interaction. This is attributable to interference between the various noncommuting terms in the total Hamiltonian (as discussed on page 141).

We summarize by comparing the expressions for the NMR time-domain signal and spectrum obtained from a time-independent Hamiltonian (Eqs. [164] and [165]) with those from a periodic Hamiltonian (Eqs. [210] and [213]): in the former case, each pair of states $\{|u\rangle, |v\rangle\}$ produces a *single* spectral peak [Fig. 11(a)], whereas in the latter case each state pair is associated with a *manifold* of spectral peaks [Fig. 11(b)]. Each amplitude $a_{uv}^{(k)}$ is the product of a_{uv} (from the time-independent case) and the Fourier component $c_{uv}^{(k)}$, as expressed by Eq. [211]. The sum over all side-band amplitudes $a_{uv}^{(k)}$ within a manifold equals a_{uv}.

SUMMARY

We have discussed a framework for calculating the NMR time-domain signal and frequency-domain spectrum generated from a single molecular orientation in solid-state NMR. The key steps are the following:

1. Construct the Hamiltonian for the spin system. This is given as a product of a spatial tensor and a spin operator, each represented by a component of an irreducible spherical tensor. We showed how the spatial tensor may be transformed between different reference frames and how the matrix representation for the spin operator may be calculated.
2. The density operator carries the information about the state of an ensemble of nuclear spin systems. The Hamiltonian will cause the density operator to change throughout the NMR experiment. The fundamental problem in spin dynamics calculations is solving the Schrödinger equation, which dictates how the spin density operator, and hence the nuclear spins, evolves in time; this results in an operator called the propagator. In practice, the propagator usually has to be estimated numerically. It may then be used to calculate the spin density operator at any time point during the NMR experiment.
3. The time-domain signal $s(t)$ at a given time point corresponds to the expectation value of an observable operator. It is calculated as the trace of the product of the observable operator and the density operator at the given time point.

By repeating the above steps for a series of time points, one obtains the time-domain signal "traject-

ory" $s(t)$. The corresponding NMR spectrum is calculated by Fourier transformation of $s(t)$. We derived the formal equations describing these steps and examined in particular detail the NMR response obtained if the spin Hamiltonian is dynamically inhomogeneous (i.e., self-commuting at all times during the NMR signal acquisition). This allowed the spin dynamics to be solved exactly. Finally, the form of the spectrum obtained from a single molecular orientation in a static and rotating sample were examined.

The next article will outline how this formalism is converted into computer code in order to numerically calculate NMR signals.

ACKNOWLEDGMENTS

I would like to thank L. Frydman, C.V. Grant, A. Sebald, and S. Vega for helpful comments on the manuscript and M.H. Levitt for many discussions and for providing *Mathematica* routines used for generating some of the figures. A postdoctoral fellowship from The Swedish Foundation for International Cooperation in Research and Higher Education (STINT) is appreciated.

APPENDIX A

We prove (i) the symmetry of the Fourier components $\omega_\Lambda^{(m)}$ upon sign reversal of m (Eq. [106]), (ii) the expression for the spatial tensor component $\omega_\Lambda(t) = [A_{20}^\Lambda]^L$ (Eq. [107]), and (iii) that the latter is real valued. These properties follow from the relationship of the irreducible spherical tensor components (Eq. [51]) and the following symmetries of the Wigner functions (*28*):

$$d^l_{m'm}(\beta) = (-1)^{m'-m} d^l_{-m'-m}(\beta) \qquad [A.1]$$

$$D^l_{m'm}(\Omega) = (-1)^{m-m'} D^l_{-m'-m}(\Omega)^* \qquad [A.2]$$

These equations may be checked explicitly using the Wigner functions given in Table 1. Substituting them into the the expression for $\omega_\Lambda^{(-m)}$ (Eq. [105]) gives

$$\omega_\Lambda^{(-m)} = \sum_{m'=-2}^{2} [A_{2m'}^\Lambda]^M \cdot \underbrace{D^2_{m'-m}(\Omega_{MR})}_{(-1)^{-m-m'} D^2_{-m'm}(\Omega_{MR})^*} \cdot \underbrace{d^2_{-m0}(\theta_m)}_{(-1)^{-m} d^2_{m0}(\theta_m)} \qquad [A.3]$$

$$= \sum_{m'=-2}^{2} (-1)^{-m'} [A_{2m'}^\Lambda]^M D^2_{-m'm}(\Omega_{MR})^* d^2_{m0}(\theta_m) \qquad [A.4]$$

where the two factors $(-1)^{-m-m'}$ and $(-1)^{-m}$ were combined into

$$(-1)^{-m} \cdot (-1)^{-m-m'} = (-1)^{-2m-m'} = (-1)^{-m'} \qquad [A.5]$$

and the last equality holds for integral values of m. After a change of index $n = -m'$, the expression for $\omega_\Lambda^{(-m)}$ is

$$\omega_\Lambda^{(-m)} = \sum_{n=-2}^{2} (-1)^n [A_{2-n}^\Lambda]^M D^2_{nm}(\Omega_{MR})^* d^2_{m0}(\theta_m) \qquad [A.6]$$

From Eq. [51] it follows that $(-1)^n [A_{2-n}^\Lambda]^M = ([A_{2n}^\Lambda]^M)^*$. Because the reduced Wigner functions are real numbers, that is, $d^2_{m0}(\theta_m) = d^2_{m0}(\theta_m)^*$, Eq. [106] follows by using standard properties of complex numbers:

$$\omega_\Lambda^{(-m)} = \sum_{n=-2}^{2} \underbrace{(-1)^n [A_{2-n}^\Lambda]^M}_{([A_{2n}^\Lambda]^M)^*} \cdot D^2_{nm}(\Omega_{MR})^* \cdot d^2_{m0}(\theta_m)^* \qquad [A.7]$$

$$= \left(\sum_{n=-2}^{2} [A_{2n}^\Lambda]^M D^2_{nm}(\Omega_{MR}) d^2_{m0}(\theta_m) \right)^* \qquad [A.8]$$

$$= \omega_\Lambda^{(m)*} \qquad [A.9]$$

Once Eq. [106] is established, it is easy to show that $\omega_\Lambda(t)$ is real: we rearrange the sum in Eq. [104] as follows:

$$\omega_\Lambda(t) = \sum_{m=-2}^{2} \omega_\Lambda^{(m)} \exp\{im\omega_r t\} \qquad [A.10]$$

$$= \omega_\Lambda^{(0)} + \sum_{m=1}^{2} \omega_\Lambda^{(m)} \exp\{im\omega_r t\} + \omega_\Lambda^{(-m)} \exp\{-im\omega_r t\} \qquad [A.11]$$

Using Eq. [106], as well as $\exp\{-im\omega_r t\} = \exp\{im\omega_r t\}^*$, we obtain

$$\omega_\Lambda(t) = \omega_\Lambda^{(0)} + \sum_{m=1}^{2} \omega_\Lambda^{(m)} \exp\{im\omega_r t\} + \omega_\Lambda^{(m)*} \exp\{im\omega_r t\}^* \qquad [A.12]$$

Note that for each value of m, we have a sum of a complex number $\omega_\Lambda^{(m)} \exp\{im\omega_r t\}$ and its complex conjugate $(\omega_\Lambda^{(m)} \exp\{im\omega_r t\})^*$; this equals 2 Re$(\omega_\Lambda^{(m)} \exp\{im\omega_r t\})$. Because it directly follows from Eq. [106] that $\omega_\Lambda^{(0)}$ is *real*, Eq. [225] corresponds to a sum of three real numbers:

$$\omega_\Lambda(t) = \omega_\Lambda^{(0)} + 2 \sum_{m=1}^{2} \mathrm{Re}(\omega_\Lambda^{(m)} \exp\{im\omega_r t\}) \qquad [A.13]$$

Finally, Eq. [107] is established by evaluating the real part of the product $\omega_\Lambda^{(m)} \exp\{im\omega_r t\}$, resulting in

$$\omega_\Lambda(t) = \omega_\Lambda^{(0)} + 2 \sum_{m=1}^{2} \mathrm{Re}\{\omega_\Lambda^{(m)}\} \cos\{m\omega_r t\} - \mathrm{Im}\{\omega_\Lambda^{(m)}\} \sin\{m\omega_r t\} \qquad [A.14]$$

APPENDIX B

Following Ref. (*36*), we show that in the Hamiltonian eigenbasis, the propagator may be expressed as a sum of products of projection operators and exponentials of dynamic phases (Eq. [145]). Here we use the shorthand notation $\Phi_u \equiv \Phi_u(t, t_0)$ and insert the expression for the dynamic phase (Eq. [143]) into Eq. [142]:

$$\hat{\mathbf{U}}(t, t_0) = \exp\left\{-i \sum_{u=1}^{\mathcal{N}} \Phi_u |u\rangle\langle u|\right\} \qquad [B.1]$$

According to Eq. [13], the propagator may be expressed as the following Taylor series:

$$\hat{\mathbf{U}}(t, t_0) = \hat{1} + \left(-i \sum_{u=1}^{\mathcal{N}} \Phi_u |u\rangle\langle u|\right) + \frac{1}{2!}\left(-i \sum_{u=1}^{\mathcal{N}} \Phi_u |u\rangle\langle u|\right)^2 + \cdots + \frac{1}{N!}\left(-i \sum_{u=1}^{\mathcal{N}} \Phi_u |u\rangle\langle u|\right)^N + \cdots \qquad [B.2]$$

We focus on the second-order term. It may be formally expressed as a sum over $\mathcal{N}^2$ products of projection operators according to

$$\frac{1}{2!}\left(-i \sum_{u=1}^{\mathcal{N}} \Phi_u |u\rangle\langle u|\right)^2 = \frac{1}{2!} \sum_{u,v=1}^{\mathcal{N}} \Phi_u \Phi_v |u\rangle\langle u| \cdot |v\rangle\langle v| \qquad [B.3]$$

This appears at first sight to be a very complex expression. However, by using the properties of "bras" and "kets" and considering that the Hamiltonian eigenstates are orthonormal, each operator product on the right-hand side may be evaluated as

$$|u\rangle\langle u| \cdot |v\rangle\langle v| = |u\rangle \cdot \underbrace{\langle u|v\rangle}_{\delta(u,\,v)} \cdot \langle v| = |u\rangle\langle v| \cdot \delta(u,\, v) \qquad [B.4]$$

The result is that $(|u\rangle\langle u|)^2 = |u\rangle\langle u|$, while all products between *different* operators vanish. This may be extrapolated to obtain the following expression for the nth-order term in Eq. [B.2]:

$$\frac{1}{N!}\left(-i \sum_{u=1}^{\mathcal{N}} \Phi_u |u\rangle\langle u|\right)^N = \frac{1}{N!} \sum_{u=1}^{\mathcal{N}} (-i\Phi_u)^N |u\rangle\langle u| \qquad [B.5]$$

It follows that *all* terms of index u in Eq. [B.2] are proportional to the projection operator $|u\rangle\langle u|$; this makes the following factorization possible:

$$\hat{\mathbf{U}}(t, t_0) = \sum_{u=1}^{\mathcal{N}} \left\{\hat{1} + (-i\Phi_u) + \frac{1}{2!}(-i\Phi_u)^2 + \cdots + \frac{1}{N!}(-i\Phi_u)^N + \cdots\right\} |u\rangle\langle u| \qquad [B.6]$$

Inspection of each term with index u in this expression within braces reveals that it corresponds to the Taylor expansion of the *exponential* function of the *number* $(-i\Phi_u)$ (see Eq. [12]). Hence, we may replace the expression within braces by $\exp\{-i\Phi_u\}$, whereupon Eq. [B.6] casts as

$$\hat{\mathbf{U}}(t, t_0) = \sum_{u=1}^{\mathcal{N}} \exp\{-i\Phi_u\} |u\rangle\langle u| \qquad [B.7]$$

which is the desired result, Eq. [145].

REFERENCES

1. Haeberlen U. High resolution NMR in solids. Selective averaging. New York: Academic; 1976.
2. Munowitz M. Coherence and NMR. New York: Wiley; 1988.
3. Ernst RR, Bodenhausen G, Wokaun A. Principles of nuclear magnetic resonance in one and two dimensions. Oxford, UK: Clarendon; 1987.
4. Schmidt-Rohr K, Spiess HW. Multidimensional solid-state NMR and polymers. New York: Academic; 1994.
5. Mehring M, Weberuß VA. Object-oriented magnetic resonance. Classes and objects, calculations and computations. London: Academic; 2001.
6. Levitt MH. Spin dynamics. Basics of nuclear magnetic resonance. Chichester, UK: Wiley; 2001.
7. Andrew ER, Bradbury A, Eades RG. Removal of dipolar broadening of nuclear magnetic resonance spectra of solids by specimen rotation. Nature 1959; 183:1802–1803.
8. Lowe IJ. Free induction decays of rotating solids. Phys Rev Lett 1959; 2:285–287.
9. Dusold S, Sebald A. Magnitudes and orientations of NMR interactions in isolated three-spin systems ABX. Mol Phys 1998; 95:1237–1245.
10. Levitt MH, Edén M. Numerical simulation of periodic NMR problems: Fast calculation of carousel averages. Mol Phys 1998; 95:879–890.
11. Charpentier T, Fermon C, Virlet J. Efficient time propagation technique for MAS NMR simulation: Application to quadrupolar nuclei. J Magn Reson 1998; 132: 181–190.
12. Hohwy M, Bildsøe H, Jakobsen HJ, Nielsen NC. Efficient spectral simulations in NMR of rotating solids. The γ-COMPUTE algorithm. J Magn Reson 1999; 136: 6–14.
13. Hodgkinson P, Emsley L. Numerical simulation of solid-state NMR experiments. Prog NMR Spectrosc 2000; 36:201–239.
14. Bak M, Rasmussen JT, Nielsen NC. SIMPSON: A general simulation program for solid-state NMR spectroscopy. J Magn Reson 2000; 147:296–330.
15. Charpentier T, Fermon C, Virlet J. Numerical and theoretical analysis of multiquantum magic-angle-spinning experiments. J Chem Phys 1998; 109:3116–3130.
16. Brinkmann A, Edén M, Levitt MH. Synchronous helical pulse sequences in magic-angle-spinning NMR. Double quantum spectroscopy of recoupled multiple-spin systems. J Chem Phys 2000; 112: 8539–8554.
17. Kubo A, Imashiro F, Terao T. Fine structures of ^{1}H-coupled ^{13}C MAS NMR spectra for uniaxially rotating molecules in deuterated surroundings: Conformations of *n*-alkane molecules enclathrated in urea channels. J Phys Chem 1996; 100:10854–10860.
18. Edén M, Lee YK, Levitt MH. Efficient simulation of periodic problems in NMR. Application to decoupling and rotational resonance. J Magn Reson A 1996; 120: 56–71.
19. Dumont RS, Jain S, Bain A. Simulation of many-spin system dynamics via sparse matrix methodolgy. J Chem Phys 1997; 106:1–9.
20. Filip C, Filip X, Demco DE, Hafner S. Spin dynamics under magic angle spinning by Floquet theory. Mol Phys 1997; 92:757–771.
21. Studer W. SMART, A general purpose pulse experiment simulation program using numerical density matrix calculations. J Magn Reson 1988; 77:424–438.
22. Skibsted J, Nielsen NC, Bildsøe H, Jakobsen HJ. Satellite transitions in MAS NMR spectra of quadrupolar nuclei. J Magn Reson 1991; 95:88–117.
23. Stickney de Bouregas F, Waugh JS. ANTIOPE, A program for computer experiments on spin dynamics. J Magn Reson 1992; 96:280–289.
24. Smith SA, Levante TO, Meier BH, Ernst RR. Computer simulations in magnetic resonance. An object-oriented programming approach. J Magn Reson A 1994; 106: 75–105.
25. GAMMA program. Florida State University, Tallahassee, FL. http://gamma.magnet.fsu.edu.
26. SIMPSON program. University of Aarhus, Denmark. http://nmr.imsb.au.dk.
27. Maricq MM, Waugh JS. NMR in rotating solids. J Chem Phys 1979; 70:3300–3316.
28. Varshalovich DA, Moskalev AN, Khersonskii VK. Quantum theory of angular momentum. Singapore: World Scientific; 1988.
29. Sakurai JJ. Modern quantum mechanics. New York: Addison–Wesley; 1994.
30. Press WH, Flannery BP, Teukolsky SA, Vetterling VT. Numerical recipes in C. The art of scientific computing. Cambridge, UK: Cambridge University Press; 1986.
31. Jeener J. Emphasising the role of time in quantum dynamics. Bull Magn Res 1994; 16:35–42.
32. Abramowitz M, Stegun IA, editors. Handbook of mathematical functions with formulas, graphs and mathematical tables. New York: Dover; 1972.
33. Vega AJ. In: Encyclopedia of NMR. New York: Wiley; 1995.
34. Farrar TC. Density matrices in NMR spectroscopy. II. Concepts Magn Reson 1990; 2:55–61.
35. Levitt MH. The signs of frequencies and phases in NMR. J Magn Reson 1997; 126:164–182.
36. Antzutkin ON. Sideband manipulation in magic-angle-spinning nuclear magnetic resonance. Prog NMR Spectrosc 1999; 35:203–266.
37. Levitt MH. Why do spinning sidebands have the same phase? J Magn Reson 1989; 82:427–433.

38. Edén M, Levitt MH. Computation of orientational averages in solid-state NMR by Gaussian spherical quadrature. J Magn Reson 1998; 132:220–239.
39. Schmidt A, Vega S. The Floquet theory of nuclear magnetic resonance spectroscopy of single spins and dipolar coupled spin pairs in rotating solids. J Chem Phys 1992; 96:2655–2680.
40. Nakai T, McDowell CA. Application of Floquet theory to the nuclear magnetic resonance spectra of homonuclear two-spin systems in rotating solids. J Chem Phys 1992; 96:3452–3465.
41. Luz Z, Poupko R, Alexander S. Theory of dynamic magic angle spinning nuclear magnetic resonance and its application to carbon-13 in solid bullvalene. J Chem Phys 1993; 99:7544–7553.

BIOGRAPHY

Mattias Edén was born in 1971 in Stockholm, Sweden. He received his B.S. in chemistry from Stockholm University in 1994 and continued there with doctoral studies in the group of Malcolm H. Levitt. Their work primarily involved pulse sequence design for determining molecular structures by solid-state NMR, as well as the development of methods for numerically simulating NMR experiments. He did postdoctoral work in the field of solid-state NMR on quadrupolar nuclei with Lucio Frydman at the University of Illinois at Chicago (2000) and at the Weizmann Institute of Science in Israel (2001). Currently, Dr. Edén is an assistant professor at Stockholm University, focusing on solid-state NMR methodology development for structural investigations of inorganic materials.